Compensation of increased passive stiffness in the ankle joint.

Design of Negative Stiffness Orthosis.

Petrus Elbertus Marie Brandjes April 22, 2016



Master of Science Thesis



Compensation of increased passive stiffness in the ankle joint.

Design of Negative-Stiffness Orthosis

MASTER OF SCIENCE THESIS

For the degree of Master of Science in Mechanical engineering at Delft University of Technology

Petrus Elbertus Marie Brandjes 1358774

April 22, 2016

Emanation committee:

Dr. Ir. Jurriaan H. de Groot Prof. Dr. Frans C.T. van der Helm Dr. Ir. Winfred Mugge Dr. Ir. Nima Tolou Dr. Ir. Erwin de Vlugt

Preface

Met veel genoegen schrijf ik het laatste stukje van mijn thesis. Met plezier kijk terug op mijn afstudeerproject en dan vooral de ontwerpfase, een oplossing bedenken die nog niet bestaat! Dagen heb ik zitten zwoegen en tobben zodat ik u uitendelijk met trots mijn thesis presenteer. De thesis beschrijft op een wetenschappelijke manier de totstandkoming van mijn afstudeerproject; the Negative Stiffness Orthosis.

Ik besef dat dit project ook het laatste is binnen mijn studie werktuigboukunde aan de TU Delft. Wat heb ik niet een plezier gehad in de intelectueele uitdaging die Werktuigbouwkunde bied! Ik prijs me gelukkig dat ik de mogelijkheid heb gehad om te studeren. En graag wil ik mijn ouders hartelijk bedanken voor deze mogelijkheid.

Tijdens mijn afstuderen ben ik ook andere mensen een woord van dank verschuldigd. Allereerst wil ik mijn afstudeerbegleider Erwin de Vlugt bedanken voor de fijne samenwerking. Het vertrouwen in mijn kunnen en positieve begleiding gedurende het project heb ik zeer gewaardeerd. Jurriaan de Groot voor zijn feedback en verrassende kijk op zaken. Vincent Mugge en Frans van der Helm voor hun bijdrage aan het eind van mijn thesis.

Mijn vrienden wil graag bedanken voor hun support tijdens mijn afstuderen. Een aantal van hen wil ik speciaal bedanken, Marijn van de Wijdeven voor zijn hulp bij het grafische gedeelte van mijn thesis, Jakko van Dijke voor de foto's en Guido Vletter voor het delen van gedachtes.

Als laatste wil ik mijn broers Bob en Jaap bedanken voor hun bijdrage en Piet en Desiree voor hun onvoorwaardelijke steun.

Pim Brandjes

Table of Contents

1.	Introduction	7
2.	Methods	14
	2.1 Working principle	15
	2.2 Patient interface and prototype.	28
	2.3 Experiment	32
3.	Results	33
	3.1 Model	33
	3.2 Prototype	33
	3.3 Case study	36
4.	Discussion	42
	4.1 Model	42
	4.2 Prototype	43
	4.3 Case study	46
	4.4 Recommendations	47
5.	Conclusion	48
6.	Reference	49
7.	Appendix A	51
8.	Appendix B	58

Abstract

This graduation project aims to develop an orthosis for patients suffering from a reduced Range of Motion (RoM) of the ankle joint. The reduced RoM is in dorsiflexion direction, the patient lacks the ability to turn the foot in the direction of the knee. This gait pattern is known as drop foot gait. This results in a low walking speed, increased energy cost and risk of falling.

The approach for the Negative Stiffness Orthosis is to compensate the increased passive stiffness of the ankle with a negative stiffness. The Negative Stiffness Orthosis(NSO) was designed, build and evaluated. Magnetic neodymium was used to generate a compensating torque-angle relation for patients with a passive ankle stiffness classified as Ashworth 2.

The novel orthosis is tested for its physical properties, the measurement of the torque-angle relation, weight and size. To test the walkability, a case study was performed on a healthy test subject.

This study suggests that this NSO potentially benefit patients with increased passive stiffness in the ankle joint during walking.

1. Introduction

This master thesis describes the development and testing of a prototype orthosis, aimed to regain motion of the human ankle joint in patients suffering from movement diseases. In this introduction I will position my graduation project in the field of existing Ankle Foot Orthoses (AFOs) and define the problem statement, approach and goals.

This graduation project aims to develop an orthosis for patients suffering from a reduced Range of Motion (RoM) of the ankle joint. The reduced RoM is in dorsiflexion direction, the patient lacks the ability to turn the foot in the direction of the knee.

Medical background

Patients with drop foot or foot equinus both suffer from reduced RoM in dorsiflexion direction. Reduced RoM for foot equinus is caused by increased stiffness in either the Achilles tendon and/or the calf or Triceps Surae (TS) muscles. In the drop foot case, the reduced RoM is predominantly caused by a weaker Tibialis Anterior (TA) muscle, due to the disuse of the ankle joint the passive stiffness increases [1,2]. Although equinus and drop foot have different causes for reduced RoM, patients experience the same problem. An increased passive ankle joint stiffness against a reduced tibialis anterior function. This results in a lack of muscle power for sufficient lifting of the foot in dorsiflexion. Lack of dorsiflexion causes inability to lift the foot adequately in swing phase. This results in a low walking speed, increased energy cost and risk of falling. This gait pattern is known as drop foot gait [3,4].

The increased passive stiffness in the ankle joint can be classified using the Ashworth Scale [5] see Figure 1.

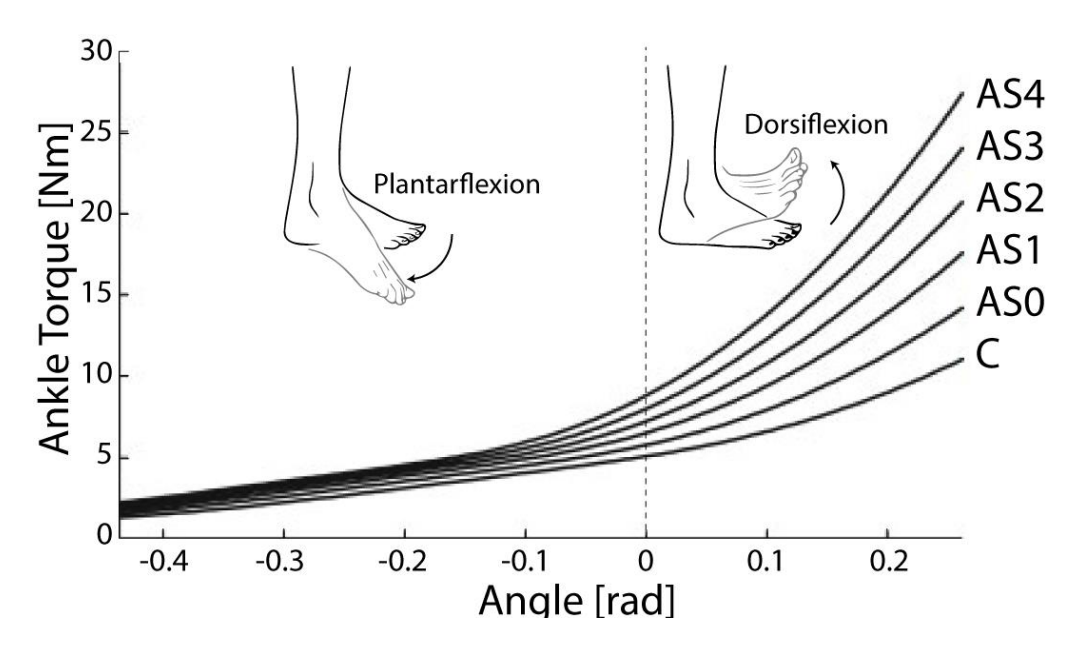


Figure 1: Torque vs angle relation for various patient groups (AS0-AS4) as well as a healthy group (C) [5]. At an angle of 0 radians the foot is perpendicular to the lower leg, positive values denote dorsiflexion direction and negative values denote plantarflexion direction.

Figure 1 shows different passive ankle stiffness of patient groups; Ashworth 4 is the severest case.

Current treatment

Current treatment for patients suffering from drop foot or equinus consists of a variety of Ankle Foot Orthoses (AFOs). AFOs are designed to help a patient achieve a better gait, increase joint stability and efficiency of walking. AFOs have 35.600 users in 2014 in the Netherlands [6]. Verbakel [7] and Shorter [8] discussed the pros and cons for the different passive AFOs. Despite various types of AFOs the approach is all the same, a positive stiffness is added to the ankle joint. The added stiffness limits the patient's RoM even further, resulting in minimal voluntary ankle movement. To get a better understanding of the problems occurring with conventional AFOs, the gait cycle for an able-bodied person is described.

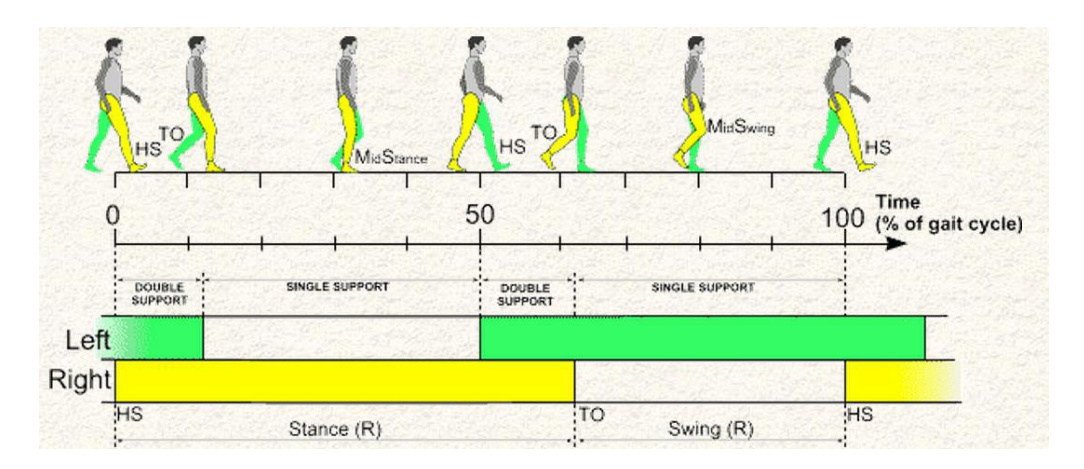


Figure 2: Gait cycle able-bodied person [9]

The gait cycle extends from Heel Strike (HS) of the right leg and includes the stance and swing phases of both legs. In the basic gait cycle there are two phases for each leg; stance phase and swing phase. The stance phase of gait can be divided into the point of initial contact, heel strike (HS), the point when the full foot is on the ground, mid stance, and the point where the stance phase ends, toe off (TO) propulsion phase. The swing phase starts at TO and ends when the foot hit the ground again HS.

A patient with limited dorsiflexion has a different gait than an able-bodied person, to realize enough ground clearance during swing phase patients tilt their hip in combination with lifting the knee, known as drop foot gait. The AFO add a positive stiffness to fixate the foot perpendicular to the lower leg. The AFO ensures that the foot is sufficiently lifted during the swing phase, to assure that the patient has enough clearance during swing phase. Due to the added stiffness, dorsiflexion and plantar flexion are now hardly possible with negative consequences for the propulsion phase and stance phase. Figure 3 shows three slightly deviant examples of AFOs, which do not add positive stiffness in two directions.







Figure 3: From left to right: DACS's AFO [10], Step Smart & Pneumaflex [11]. The three orthoses all add a positive stiffness to prevent plantarflexion while dorsiflexion is not hampered by any stiffness. From left to right different mechanisms are responsible to realize the stiffness; metal spring, rubber-like blocks and a pneumatic jack.

The common character of these three AFOs is that stiffness is not added in both dorsiflexion direction and plantarflexion direction. Stiffness is only added to prevent plantarflexion to realize the needed clearance during swing phase. The patient would still be able to move in dorsiflexion direction which can be beneficial for the gait pattern in stance phase. The patient has a decrease in RoM, moving in plantar flexion is hindered by the counterforce of the several types of spring-like systems.

The downfall of these AFOs is clear; the movement of the patient is constricted by the non-articulated passive orthoses. The limit in Range of Motion due to the AFO has a purpose, the patient is provided with foot clearance during swing phase. The price of this foot clearance is high; Patient RoM decreases, propulsion phase is hampered, stance phase is hampered and extra weight is added to the leg of the patient. The treatment of drop foot by current AFOs is far from ideal, therefore another approach is necessary.

Negative Stiffness Orthosis

The approach for the Negative Stiffness Orthosis (NSO) is radically different. The goal is to increase range of motion in dorsiflexion direction of the patient. This is done by compensating the increased passive stiffness of the ankle with a negative stiffness. The patient can now move his ankle with very little force left in his Tibialis Anterior muscles. A schematic representation in Figure 4 shows a comparison between the four different cases: healthy control, patient, patient wearing an AFO and a patient wearing a NSO.

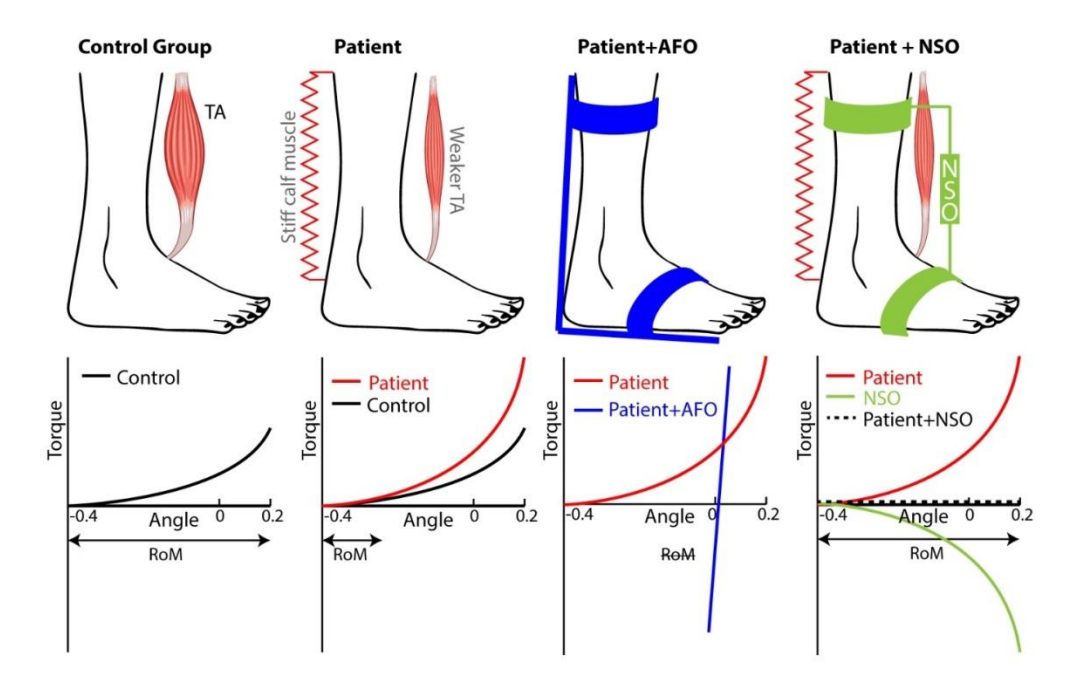


Figure 4: A schematic representation of 4 cases from left to right: Healthy Control, Patient, Patient + AFO and Patient + NSO. For each case the lower leg is shown with according passive torque vs angle relation of the ankle joint. In the case of a patient the red spring-like element represents the increased stiffness in the calve muscles, the smaller Tibialis Anterior represents the decrease in muscle force in patients. In the case the patient wears an AFO the blue line represents the high stiffness imposed by the AFO resulting in zero Range of Motion. In the case of the NSO the NSO is represented as a 'black box', resulting in a dashed line for the passive torque vs angle relation.

The Negative Stiffness Orthosis (NSO) balances increased passive tissue elasticity in the patient's ankle. The positive torque vs angle relation in the ankle joint is compensated by the negative torque vs angle relation of the NSO. The dashed line at the right graph in Figure 4 indicates the balanced torque vs angle relation for the patient. Physically the foot can now be moved with very little torque, the only torque needed is to overcome friction. The ankle has adapted into a system operating at a lower net potential energy due to the balance between the passive joint stiffness and the NSO.

An NSO would allow the patient to move in dorsiflexion direction with even the slightest force left in his tibialis anterior muscles. In an ideal case the NSO increases RoM resulting in enough clearance during swing phase while the ability to apply plantar flexion movement for propulsion remains.

Results Negative Stiffness Orthosis

Two thesis projects by Verbakel [12] & Derks [13] have been devoted on the effects of negative stiffness compensation [13] and resulted in a prototype NSO [12]. The first prototype NSO has been developed by Verbakel [12] in 2013. The

NSO prototype weighs 3.5 kilogram and is too heavy and bulky to wear during walking. The validation of the NSO prototype shows a positive perspective for further development of the NSO. Derks [13] shows that negative stiffness enables a larger active dorsiflexion RoM than in the situation without compensation, using the same muscular activation. Derks [13] showed that negative stiffness has a positive effect on active RoM, especially in dorsiflexion.

The current results show that the patients can have a better range of motion but only in a controlled and sedentary position. However, it remains to be proven to what extent the increased ankle RoM leads to improvements during walking.

Patients can be graded according to their passive stiffness on the Ashworth scale. Every patient has its own torque-angle relation, therefore an orthosis must be an individualized device. In this study the AS2 patient group is of our interest, if the NSO can compensate for AS2 patients it implies that it can compensate AS1 and AS0. AS2 torque-angle relation represents a group of patients were muscle force in the TA is present where for patients with AS3 and AS4 this is questionable. The NSO does not contribute to an increase in RoM for Patients without muscle force in the TA. The AS2 torque-angle relation must be seen as a guideline to prove that compensating this torque is possible in a NSO. The compensating Negative Ashworth 2 (NAS2) is the torque vs angle relation to be achieved by the NSO, in Figure 5 the NAS2 is plotted.

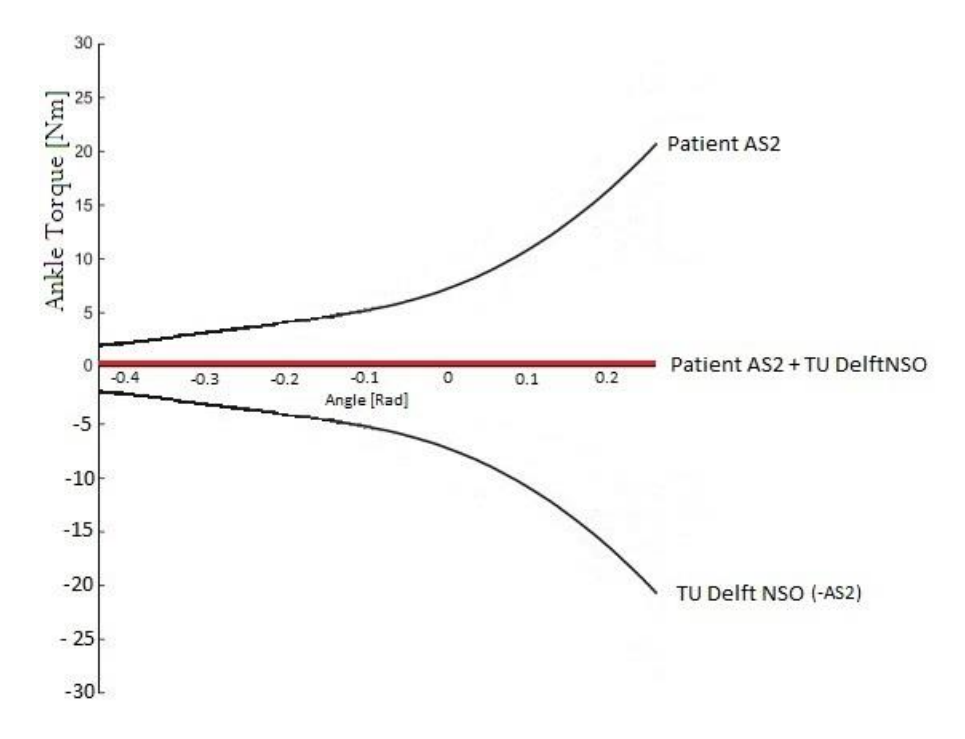


Figure 5: Torque-angle relation for patient AS2 and NSO [5]. At an angle of 0 radians the foot is perpendicular to the lower leg, positive values denote dorsiflexion direction and negative values denote plantarflexion direction. The red line is the result of the summation of the AS2 and the NSO.

Problem statement

A Patient diagnosed with equinus or drop foot lacks muscle force to overcome increased passive stiffness in ankle joint, this results in insufficient gait.

Objective

Design, build, test and evaluate a novel Negative Stiffness Orthosis which is suitable for walking conditions with an NAS2 torque vs angle relation. This thesis aims to fulfill the requirements of 1) controllability (lightweight and walkable) and 2) sufficient comfort for endured use. Cosmetics are beyond the scope of the thesis in order not to impose too many design constraints in the limited time available.

Master thesis

The first part of the thesis is to explore the possibility of using neodymium magnets as the favored energy storage material to create the target NAS2 torque-angle relation. In this proof of principle, a model of a mechanism is made, the mechanism transforms the force distance relation of the magnetic neodymium into the NAS2 torque-angle relation.

The proof of principle results in dimensions of the magnet and placement of the neodymium magnets on the NSO. The design of the NSO is explored based on the model described in the first part of the thesis. The second part describes the fabrication of the prototype NSO.

The last part of the thesis is to test the prototype. The novel orthosis is tested for its physical properties, the measurement of the torque-angle relation, weight and size. To test the walkability, a case study was performed on a healthy test subject. The effect of different levels of applied negative stiffness on a healthy person's gait is investigated.

2. Methods

The design of the NSO is split up in three sub-functions:

1. Energy storage

The NSO uses the magnetic material neodymium to provide the work needed for the NAS2 torque-angle relation. The magnetic energy source will transfer potential energy into a force acting over a distance, the force-distance relation.

2. Transformation

The function of the transformation mechanism to transform translation into rotation. In terms of forces the force-distance relation of the magnetic material needs to be transformed in the NAS2 torque-angle relation.

3. Patient interface

The NSO will have the NAS2 torque-angle relation that needs to be transferred to the patient. The NSO needs to be firmly attached to be sure that the foot does not move inside the NSO.

The energy storage sub function off the NSO was the subject of my literature study. The literature study is titled: "Energy storage in negative stiffness orthosis" [14]. The goal for this literature research is to compare different forms of storage of potential energy. In the previous prototype [12] a spring was used for energy storage, a spring has a non-ideal force distance relation. The use of a spring resulted in a bulky and heavy prototype. The type of potential energy storage is crucial for the design of the NSO. In this assessment the systems were compared against factors that are useful for the NSO. Two obvious important factors of the energy source are specific energy (energy/mass) and energy density (energy/volume).

Table 1: 3 different forms of potential energy compared: Elastic energy, molecular energy and magnetic energy. The table shows the specific energy and energy density for each potential energy source.

	Specific energy <u>J</u> kg	Energy density <u>MJ</u> m ³
Polyuret hane	$3188 \frac{J}{kg}$	$\frac{m}{37 \frac{MJ}{m^3}}$
Steel	$135 \frac{J}{kg}$	$1.06 \frac{MJ}{m^3}$
Air spring	$91\frac{J}{kg}$	$0.35 \frac{MJ}{m^3}$
Magnet	$11\frac{J}{kg}$	$0.08 \frac{MJ}{m^3}$

In Table 1 several sources of potential energy are compared for specific energy and energy density. Polyurethane has the highest specific energy and energy density and is a positive stiffness system. The prototype [12] was an example that a positive stiffness system results in a heavy and bulky design. The second disadvantage of hysteresis in Polyurethane resulted in the choice of neodymium for the energy storage in the NSO. The energy used for patient group AS2 is 3.8125 Joules. To store 3.8125 Joules in potential energy 347 grams of neodymium is needed, which is an acceptable weight for the application being an AFO.

The Methods Section consists of 3 sections:

- Section 2.1: Working principle, is about realizing a theoretical working principle to generate the NAS2 torque-angle relation with the use of the magnetic Neodymium as energy storage.
- Section 2.2: Describes the realization of the prototype based on the theoretical working principle presented in Section 2.1.
- Section 2.3: Evaluation of the prototype. Explains the experimental set up to test the NSO physical properties and the measurement of EMG in a walking test.

2.1 Working principle

The first step is to explore the possibility of using magnetic neodymium to create the NAS2 torque-angle relation. The working principle covers both the energy storage and the transformation sub functions.

Sub function 1: Energy Storage

The first sub function is the energy storage for the NSO. Based on the literature study by Brandjes [14] the material used for energy storage is the magnetic material neodymium. The electromagnetic energy or electromagnetic force field results in two bodies having interaction forces without physical contact. The potential energy storage is most beneficial with two magnets facing each other with opposite poles. Magnets with opposite poles exert an attraction force at each other. The maximum force is reached when the magnets are closest to each other. The attraction force is zero when the magnets are separated and the electromagnetic force field is out of reach. The properties of the force field, as being the excited forces, have an increasing non-linear force distance relation. The potential energy is stored when two magnets are separated. The amount of potential energy equals the line displacement integral of exited attraction force against distance.

In the configuration of two magnets facing each other with opposite poles the material neodymium can store has a specific energy of 11 joule per kilogram [14]. The amount of energy to compensate the patient with AS2 is 3.8125 Joule [14]. The weight for the magnet material neodymium becomes: $\frac{3.8125 \ [Joule]}{11 \ [\frac{Joule}{kg}]} = 347 \ Grams \ .$

Magnet dimensions

The magnetic neodymium is available in a wide variety in size and weight. The approximate weight of the needed neodymium is 347 grams, but the according dimensions need to be determined.

The dimensions influence different factors: force distance relation and energy storage (amount of potential energy stored per kilogram of neodymium).

The aim for the factor energy storage is to find magnet dimensions with a maximum amount of energy storage. The cylinder magnet S-20-10-N weighs 24 grams has a diameter of 20 mm and a thickness of 10 mm [15]. Compared to other magnets it is the magnet with the highest specific energy. This magnet had a maximum attraction force of 122 Newtons and according to the datasheet the attraction force approaches zero for a distance of 15 mm between the two magnets. The magnet S-20-10-N is the magnet with the highest energy storage [41] and is the magnet that is chosen as energy storage for the NSO.

Magnet properties

The magnet with number S-20-10-N [15] is used to conduct the NSO. The dimensions are known, as well as the weight and the force distance relation. There are many properties that influence the performance of the magnet as energy storage. The following properties appear relevant for the application at hand:

- Magnets work with the principle of superposition. The principle of superposition for the magnets is advantageous, for the practical implementation there is no need to investigate the magnets configuration in relation to each other.
- Magnet to magnet attraction does not have the disadvantageous effect of hysteresis. It means that there are no energy losses in the form of hysteresis.
- Demagnetization is the reduction or elimination of magnetization leading to a reduction in the magnetic attraction forces. Neodymium magnets are known for their low level of demagnitization. If the magnets are not overheated or physically damaged neodymium magnets will lose less than 1% of their strength over 10 years [16]. Nor will neodymium magnets lose strength if they are held in repelling or attracting positions.

The force-distance relation for magnet to magnet attraction was determined in a position-controlled test on a draw bench. In this test the absence of hysteresis is verified as well. A schematic representation of the test is provided in Figure 6.

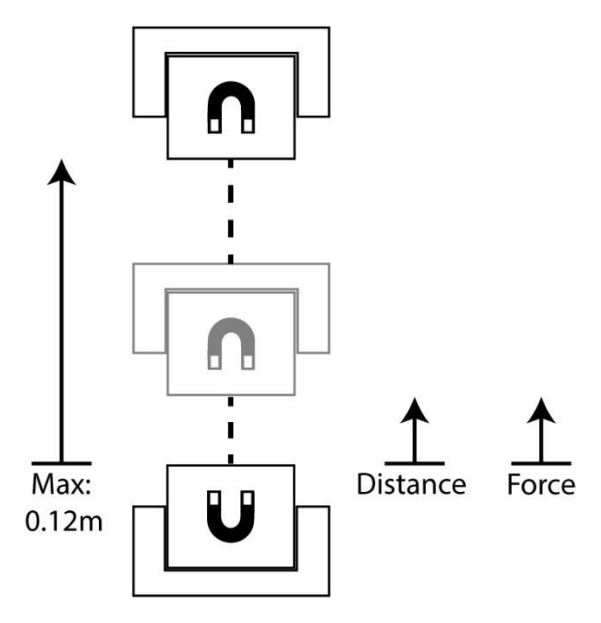


Figure 6: Schematic representation of the magnets put in a draw bench. The draw bench is position controlled and the magnets are separated for a maximal distance of 0.12 meter. The direction of the arrows of force and distance denote the positive values for both.

The magnet is hold into place by a handmade aluminum clamp (aluminum does not influence the magnetic field). The magnet above travels from a distance of 1200 mm between the two magnets to a distance of 0 mm between the magnets. The test has been done repeatedly with a cycle of 100 times. Also a comparison is made between an iron mockup, with the same size, and a magnet. For a power-to-weight ratio the magnet outperforms the magnet-to-iron combination.

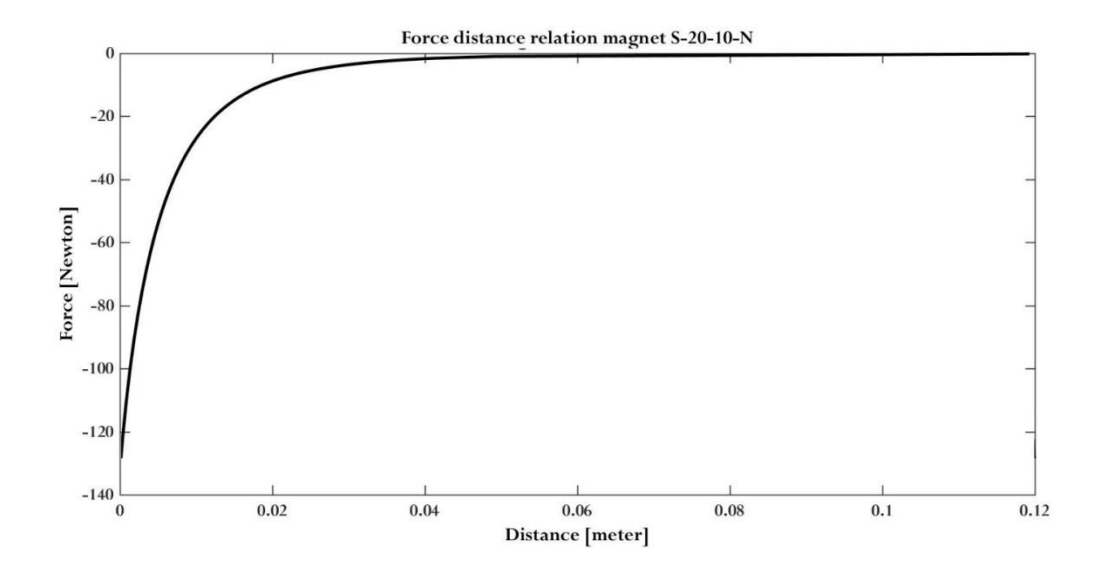


Figure 7: The force-distance relation for the magnet (S-20-10-N) to magnet attraction. The black line represents the attraction force for one cycle, starting from 0 meter to 0.12 meter and back to 0 meter.

Figure 7 is the result of a position-controlled path with the magnet traveling from zero to 0.12m and back to the zero position the attraction force is measured during the test. With force on the vertical axis it can be seen that beyond 0.04 m the magnets start to exert attraction forces. At a slight distance (0.8 mm) that separates the magnets from touching, the maximal attraction force was 126 N. There is no hysteresis, the black line in Figure 7 shows that the lines perfectly match. The force-distance relation did not change after 100 cycles The line displacement integral of the line in Figure 7 determines that the energy storage for the measurement of the two magnets is: 0.83 Joule. The weight of the 2 magnets is 0.048 grams so the specific energy for the two magnets is $\frac{0.83[Joule]}{0.048[Kilogram]} = 17.38 \frac{Joule}{kg}$ That means that the theoretical approximation was too low with 11 Joule/kg. The expected weight of magnetic material is now less than 347 grams: $\frac{3.8125\ [Joule]}{17.38\ [\frac{Joule}{kg}]} = 220\ Grams$

The measured force-distance in Figure 7 are estimated by a function where force depends on distance. This 10th order function is described the Equation 2.1. The function is fitted with matlab with the norm of residuals of 1.211:

$$Force(s) = 3.6125 \times 10^{18} \times s^{10} - 6.4421 \times 10^{17} \times s^9 + 4.8791 \times 10^{16} \times s^8 - 2.038 \times 10^{15} \times s^7 + 5.1099 \times 10^{13} \times s^6 - 7.8355 \times 10^9 \times s^5 + 7.173 \times 10^9 \times s^4 - 3.5982 \times 10^7 \times s^3 + 8.789 \times 10^4 \times s^2 + 75.604 \times s + 1.6542 \quad \text{Eq. 2.1}$$

Sub function 2: Transform translation into rotation

The aim of sub function 2 is to create the NAS2 torque-angle relation with the magnet [15] as energy storage. In terms of movement this is the transformation from translation into rotation. In term of forces the sub function transforms force into torque.

There are strict input and output parameters to be met by the sub function, summarized in figure 8.

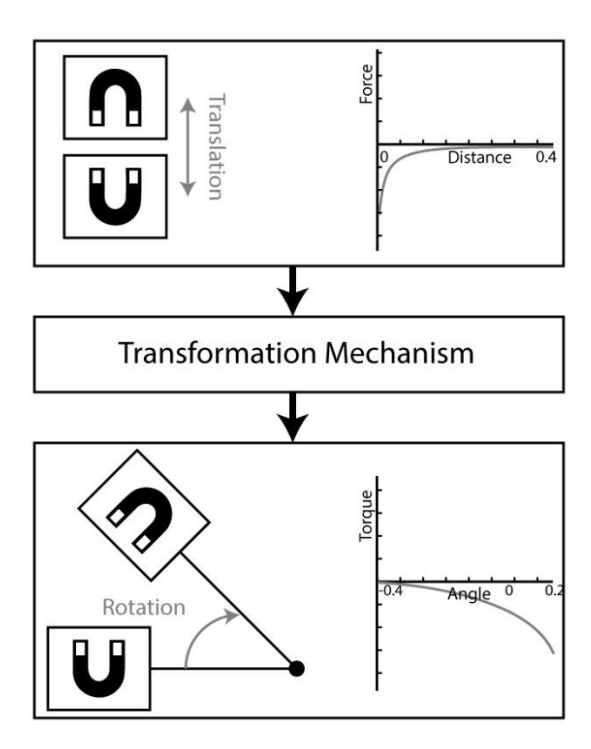


Figure 8: Illustration of transformation mechanism. Above are the properties of the translation of the magnets with the according force-distance relation. The transformation mechanism must transform this translation into rotation and in the NAS2 torque-angle relation.

Figure 8 illustrates the input parameters versus the goal as being the output parameters.

$$Torque(\theta) = -1 \times (62.5 \times \theta^4 - 29.672 \times \theta^3 + 17.405 \times \theta^2 \ 2.2123 \times \theta + 1.372)$$
 Eq 2.2

The function NAS2 plotted in Figure 3, can be described by Equation 2.2. The torque depends on input angle θ .

Model transformation mechanism

A simple 2-bar mechanism transforms translation into rotation. On each bar one magnet both at a certain length of the pivot point. The two magnets will exert an attraction force resulting in a torque acting around a pivot point. In a schematic presentation:

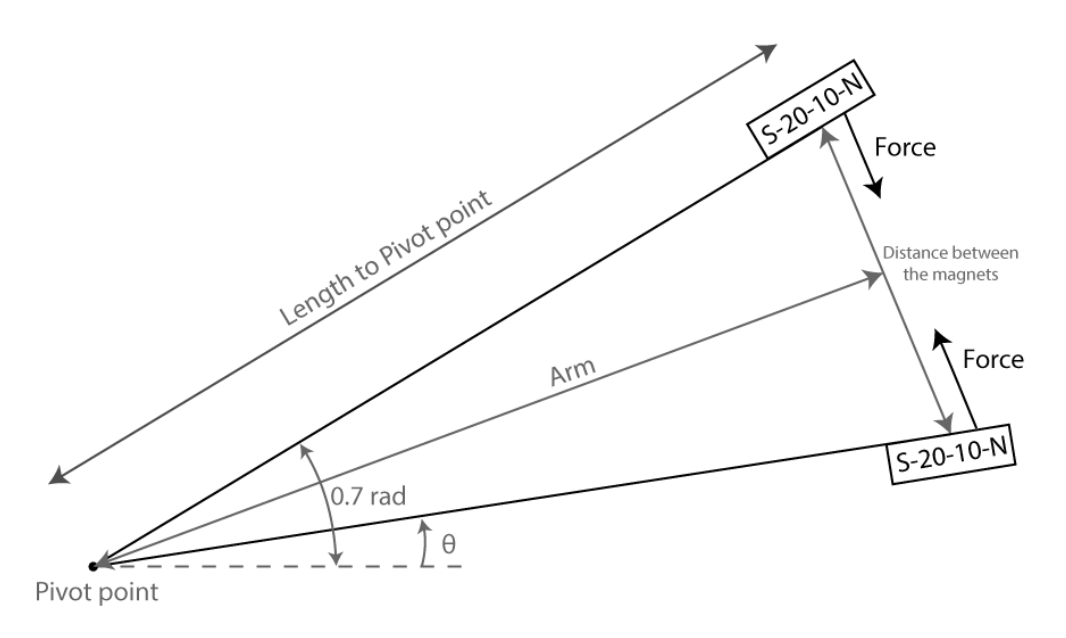


Figure 9: Sketch of a simple model with two S-20-10-N magnets. Two magnets are put at the same length on two different beams, with the magnetic attraction force they create a torque around the pivot point. The angle for maximum separation for the magnets is 0.7 radians.

Figure 9 shows that the mechanism in combination with two neodymium magnets S-20-10-N transforms force into torque. Figure 5 shows that the range of the NAS2 in terms of rotation angle is 0.7 rad. The maximum angle for the mechanism is therefore chosen to be 0.7 rad. The magnet has an effective force field from 40 mm to 0 mm of separation. For the maximum angle being 0.7 rad and the maximum distance 40 mm between the magnets the length of the

magnet to the pivot point is calculated:
$$\frac{\frac{0.04}{2}}{\sin(\frac{0.7}{2})} = 0.058 \text{ meter}$$

The distance from the center of the magnet to pivot point (length PP) is 0.058 meter. The formula for torque is given by Equation 2.3.

$$Torque(\theta) = Force \times Arm$$
 Eq 2.3

In Equation 2.3 the variable Force is the amount of attraction force between the two magnets, Arm is the length perpendicular to the direction of the force to the pivot point, see Figure 8. The distance between the two magnets can be written as a function of the angle (θ) :

$$Distance(\theta) = 2 \times (0.058 \times \sin(\frac{\theta}{2}))$$
 Eq 2.4

The arm can be expressed as function from (θ) as well:

$$Arm(\theta) = (0.058 \times \cos(\frac{\theta}{2}))$$
 Eq 2.5

The attraction force exited by the magnets depends on the distance between the two magnets. Distance is described as function of (θ) by Equation 2.4. Force is described as a function of distance in Equation 2.1. Force can be described as function from (θ) , by replacing the variable s by distance as described in equation 2.4. With force (θ) and $arm(\theta)$ known the torque now depends solely on the angle (θ) .

$$Torque(\theta) = Force(\theta) \times Arm(\theta)$$
 Eq 2.6

Equation 2.6 is rewritten by replacing the variable Force by equation 2.1 and the variable Arm by Equation 2.5:

$$Torque(\theta) \\ = \{3.6125 \times 10^{18} \times [2 \times (0.058 \times \sin(\frac{\theta}{2}))]^{10} - 6.4421 \times 10^{17} \\ \times [2 \times (0.058 \times \sin(\frac{\theta}{2}))]^9 + 4.8791 \times 10^{16} \times [2 \times (0.058 \times \sin(\frac{\theta}{2}))]^8 - 2.038 \\ \times 10^{15} \times [2 \times (0.058 \times \sin(\frac{\theta}{2}))]^7 + 5.1099 \times 10^{13} \times [2 \times (0.058 \times \sin(\frac{\theta}{2}))]^6 \\ - 7.8355 \times 10^9 \times [2 \times (0.058 \times \sin(\frac{\theta}{2}))]^5 + 7.173 \times 10^9 \\ \times [2 \times (0.058 \times \sin(\frac{\theta}{2}))]^4 - 3.5982 \times 10^7 \times [2 \times (0.058 \times \sin(\frac{\theta}{2}))]^3 + 8.789 \\ \times 10^4 \times [2 \times (0.058 \times \sin(\frac{\theta}{2}))]^2 + 75.604 \times [2 \times (0.058 \times \sin(\frac{\theta}{2}))] + 1.6542\} \\ \times (0.058 \times \cos(\frac{\theta}{2})) \\ Eq. 2.7$$

Equation 2.7 gives us the torque-angle relation for 2 magnets on the lever mechanism in Figure 9.

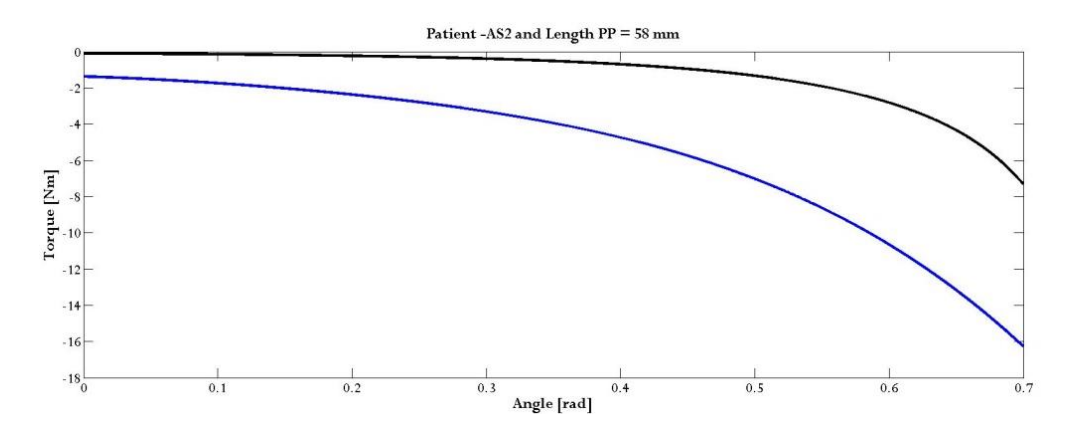


Figure 10: Torque-angle relation (Eq 2.7) with 2 magnets at Length PP= 58mm and NAS2 (blue line).

The torque-angle profile for Equation 2.7 is compared to the NAS2 profile in Figure 10. The NAS2 profile has a lower torque-angle relation with a different shape. It means that more potential energy is needed to reach the NAS2 profile. For small angles, the torque is low and when the angle approaches 0.7 rad the torque increases rapidly, the torque at 0.7 rad is more than double the torque at 0.6 rad. The NAS2 torque-angle relation increases less than 50% from 0.6 to 0.7 rad.

The transformation mechanism successfully couples the force-distance relation into an appropriate torque-angle relation. The lever mechanism does not succeed in realizing the same shape in torque-angle relation as the NAS2 torque-angle relation. Equation 2.7 learns that for a given magnet [15] force and arm depend on two input parameters the angle θ , and the chosen length from magnet to pivot point, Length PP. That means that torque depends on angle θ , and the length from magnet to pivot point, Length PP.

Shaping torque-angle relation by changing the length from magnet to the pivot point.

In Equation 2.7 is seen that torque depends on the chosen Length PP. Length PP of 58 mm is determined for the maximum length of the force field of the magnet (translation) and the needed working angle (rotation). The needed working angle is pre-determined and is 0.7 rad. The Length PP does not have to be 58 mm the length can be chosen to be shorter or longer. The torque-angle relation will change by changing the length from the magnet to the pivot point. How does the variable Length PP influence the torque-angle relation?

Shorter Length PP

For a shorter Length PP the arm is shorter and therefore the expectation is that the maximum torque is lower. A shorter Length PP is expected to result in torque increasing slowly for increasing angle. Due to the fact that the path travelled by the magnet is shorter than it's full length working force field. The expectations can be verified by the first example:

Length PP is chosen to be small; 10 mm. For a the maximum angle of 0.7 rad the distance between the two magnets becomes: $2 \times \left(0.01 \times \sin\left(\frac{0.7}{2}\right)\right) = 0.0069$ meter. Figure 7 shows that the attraction force, for the magnets separated at a distance of 7 mm, is about 60 N. So over the full angle of 0.7 the minimum force is only about half the maximum force of 126 N. The maximum torque is $0.01 \times 126 = 1.26$ Nm, in comparison the torque in Figure 10 is 7 Nm. In Figure 11 the torque-angle relation is plotted for a Length PP of 0.01 meter. In conclusion the expectations are met; the minimum force is only half the maximum force and the maximum torque is indeed lower.

Longer Length PP

The expectation for a longer Length PP is that the force increases rapidly in a small range of the rotational angle. For a longer Length PP a higher maximum torque is expected due to the length of the arm. The expectations can be verified by a second example:

The Length PP is 100 mm, the distance between the magnet at the minimum angle is: $2 \times \left(0.1 \times \sin\left(\frac{0.7}{2}\right)\right) = 0.069 \, \text{meter}$ at this distance the attraction force is 0 newton. For an angle of 0.4 radians the distance is: $2 \times \left(0.1 \times \sin\left(\frac{0.4}{2}\right)\right) = 0.04 \, \text{meter}$. For an angle smaller than 0.4 the magnets are at a greater distance than 40 mm and therefore F \approx 0 and thus T \approx 0. So in other words I expect the Torque to be 0 for $\theta < 0.2$. The torque will go from zero to maximum torque $0.1 \times 126 = 12.6$ Newton in 0.3 radians of rotational angle. As expected this results in a high ramp for the torque and a relative higher maximum torque.

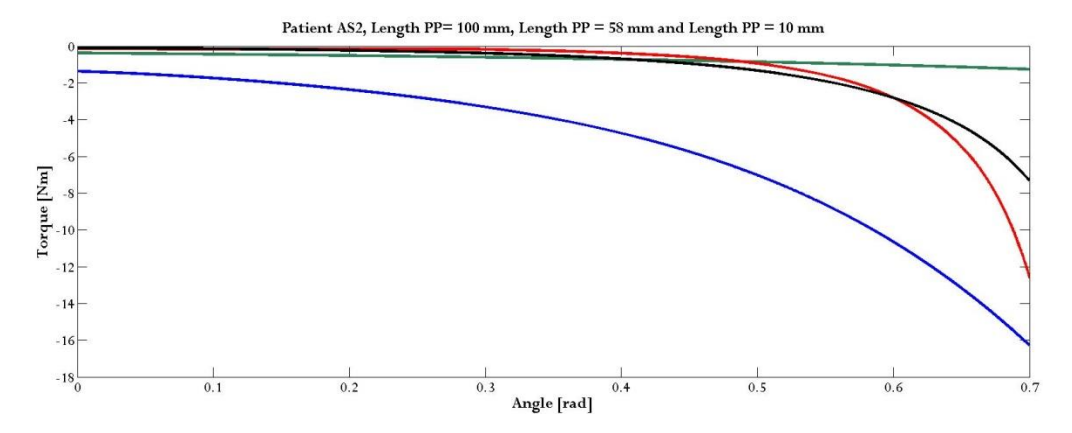


Figure 11: Torque-angle relation: NAS2 (blue line) compared with the three examples Length PP=0.01(green line), Length PP=0.058 (black line) and Length PP=0.1(red line)

Figure 11 shows the green the line for the case Length PP=0.01 meter. As expected the torque decreases for θ getting bigger while the decrease in torque is not as drastic. As expected the red line (Length PP = 0.1) equals zero for θ smaller than 0.2. The torque increases from 0 to 12.6 Nm when the θ >0.2. The maximum torque is influenced as expected, the longer Length PP the higher the maximum torque. Figure 11 shows that for θ < 0.4 rad the Length PP=0.01 has the highest torque. The blue line is the reference line NAS2, this was plotted to put the other torque-angle relations into perspective. The shape of torque-angle relation of the simple lever mechanism can be tuned by changing the length from the magnet to the pivot point. The factor, Length PP, is compared and seems to be promising in terms of realizing different relations of torque and angle. To be able to realize the NAS2 torque-angle relation an increase in amplitude is needed. The increase in amplitude can be realized by increasing the amount of magnets, the magnets weigh 48 grams in total where 220 grams of magnets is needed.

Energy efficiency influenced by length from magnet to pivot point

The energy efficiency is defined as: $\frac{Work}{energy\ available} = efficiency$.

In the first example for Length PP=0.01 the maximum distance the magnets separate is 0.0069 meter. The amount of work done by the magnet is less, decreasing the efficiency:

The working field in this cases reaches from 0 mm to 6.8 mm instead of the full range which reaches from 0 to 0.04. When the magnet is not separated up to that maximum 0.04 working length it is not used up to its full capacity. For the Length PP=0.01 the work done is 0.4914 Joule see Appendix A for the calculations, the capacity for a set of magnets [21] is 0.8342 Joule. The efficiency is calculated to be:

 $efficiency = \frac{0.49141 \, Joule}{0.8342 \, Joule} = 58.91 \, \%$

When the magnets are positioned closer to the pivot point than 58 mm the magnets are separated to their full length force field. Due to this effect the energy efficiency is less than 100 % for Length PP<0.058 meter.

Increasing amplitude of torque-angle relation by using multiple magnets

Figure 11 shows that the shape can be changed by changing the length to the pivot point. Figure 11 shows also that an increase in amplitude is needed. To realize this increase multiple magnets are needed. The placing of multiple magnets at the same Length PP is called parallel placement of the magnets. The placement of multiple magnets at different Length PP is called series placement of the magnets. In the Figures 12,13 and 14 the torque-angle relation is plotted for 3 Length PPs in parallel placement.

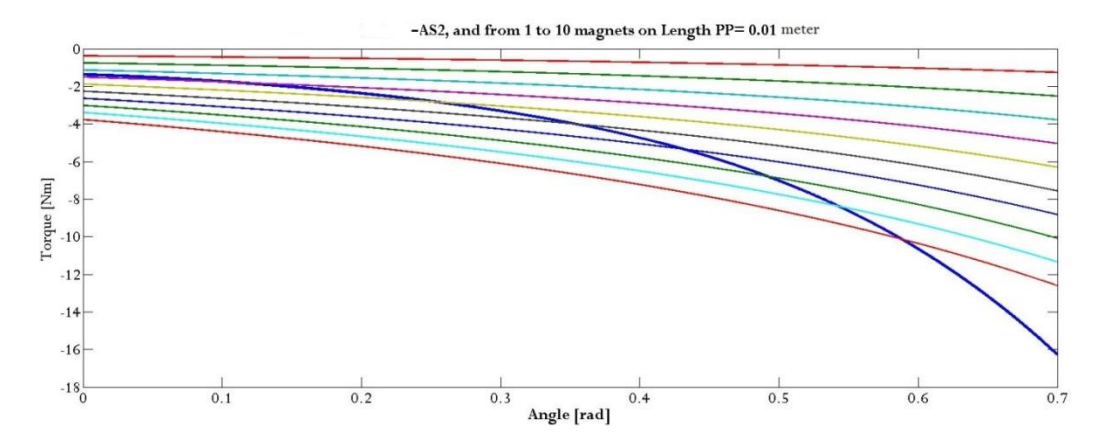


Figure 12: Length PP=0.01 from 1 to 10 magnets in parallel configuration NAS2(blue line).

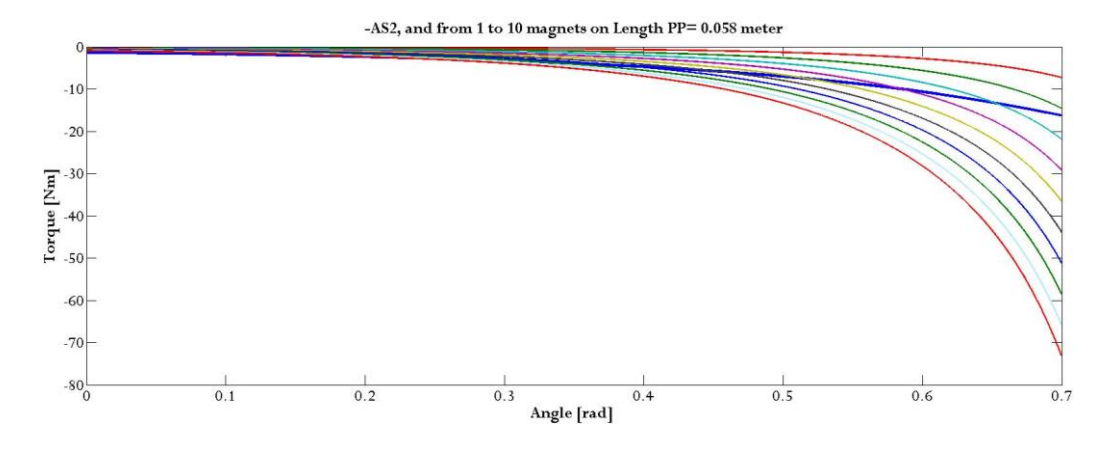


Figure 13, Length PP=0.058 from 1 to 10 magnets in parallel configuration NAS2(blue line).

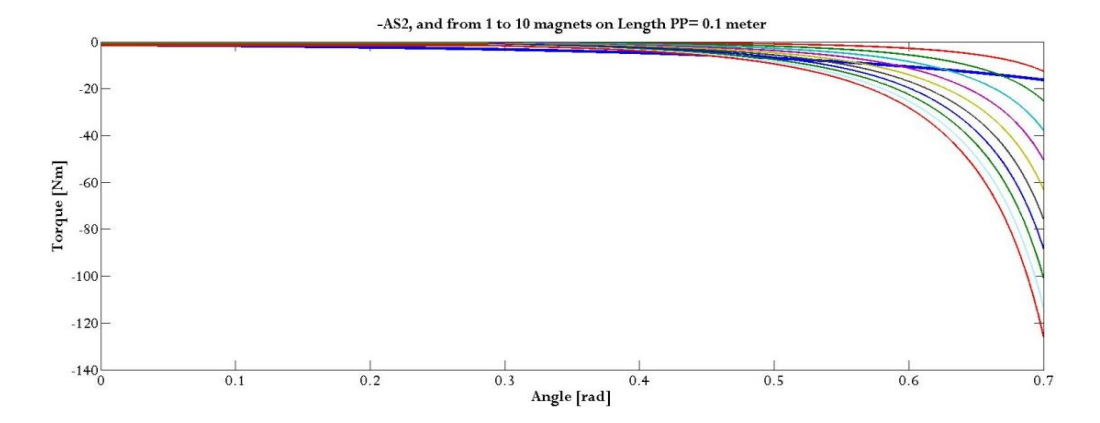


Figure 14: Length PP=0.1 from 1 to 10 magnets in parallel configuration. NAS2(blue line)

Figure 14 shows that the torque-angle relation for 10 magnets has a lower torque than the NAS2 for angle <4.5 rad. The maximum torque for Figure 14 is 126.1 Nm where 16.3 Nm needed for the NAS2 torque-angle relation. Figure 12 shows the opposite, for 10 magnets at Length PP the maximum torque is lower than NAS2 torque-angle relation whereas for angle <0.58 rad the torque is higher than NAS2 torque-angle relation. Figure 13 shows that for angle >0.2 rad the torque is higher than the NAS2 profile for 10 magnets in parallel, the maximum torque is already surpassed when 3 magnets are in parallel.

The examples plotted in Figures 12,13 and 14 show that the different mechanisms are able to reach the amount of torque for small and big angle. The problem is to match the shape of the required NAS2 torque-angle relation over the entire RoM.

Effects magnet in series and parallel.

To solve the problem of reaching the shape of the NAS2 torque-angle relation two factors can be used. The first factor is the series placement of the magnets, this factor influences the shape of the torque-angle relation. The second factor is the parallel placement of multiple magnets this increases the amplitude of the torque-angle relation.

Series:

Shorten arm

- Lower maximum Torque
- Ratio between lowest and highest torque decreases.
- Slope decreases.
- For Length PP shorter than 0.58 efficiency decreases.

Lengthen arm

- Higher maximum torque
- The slope increases
- For Length PP shorter than 0.058 efficiency increases

Parallel

Increases torque with a factor off the torque-angle relation for the chosen Length PP.

Design Criteria for transformation mechanism

The main objective for the transformation mechanism is to transform the force distance relation into the NAS2 torque-angle relation. The combination of series configuration and parallel configuration of the magnets, can realize the NAS2 torque-angle relation. The specific configuration of magnets influences the efficiency and the dimensions.

The criteria to reach the NAS2 torque must be below a margin lower than 1 Nm. The Length PP must be smaller than 0.1 meter and bigger than 0.01 meter, this is to limit the size of the prototype. The aim is to keep efficiency as high as possible and weight as low as possible.

Transformation mechanism

Appendix A shows the description of the model of the mechanism in Matlab. In this model the Length PP can be varied easily. The number of magnets can be chosen according to the Length PP. The third factor being efficiency is an output for the configuration of the magnets.

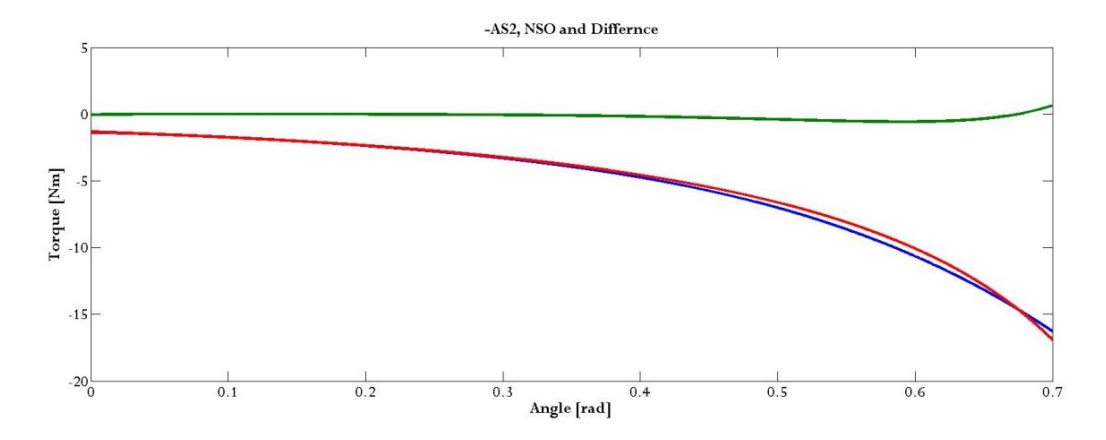


Figure 15 shows, the NAS2 torque-angle relation (blue line), the NSO torque-angle relation (red line) and the difference between the NAS2 and the NSO torque-angle relation.

Figure 15 the NSO is compared with the NAS2 profile with a resultant torque that must have a lower absolute value than 1Nm. The configuration with Length PP1= 18 mm, Length PP2= 20 mm, Length PP3 = 27 mm, Length PP4 = 28 mm and Length PP5 = 42mm with according efficiency of 88.31%. For this configuration the NSO is matched with the NAS2 within 1Nm margin.

2.2 Patient interface and prototype.

Patient interface

The last sub function is transfer the torque of the mechanism and magnet to the patient. This subfunction does not require a new design. There are existing orthoses with a standard comparable shape and function. The use of the same type of shell is favorable, because it is widely used and fully developed. To solve this last subfunction a more practical approach is needed.

This practical approach consisted of informative meetings with people from Noppe Orthopedics. Noppe Orthopedics is company that builds various types of AFOs. The type of shell was determined for the NSO prototype with help of their knowledge.

The orthosis has two Otto-Bock hinges at the ankle joint to assure stability for the NSO. A stainless steel piece is designed to fit the Otto-bock hinges. This stainless steel piece fits in the shoe part of the NSO and is responsible for transferring the force of the magnets to the shoe part of the NSO.

An aluminum t-profile attached to the shin part of the NSO. The magnets were bolted on the aluminum profile to transfer the forces to the shin part of the NSO

Manufacturing Prototype

The prototype was built in the workshop of Noppe Orthopedics. The prefabricated pieces and Otto-Bock hinges can be seen in Figure 16.



Figure 16, the prefabricated pieces. The two Otto-bock hinges at the bottom right side. The two stainless steel pieces to fit in the shoe side of the orthosis are shown above in the figure. The aluminum pieces are at the bottom left side, clay is added to prevent adhesion of epoxy raisin.

The NSO was made according to the size and shape of my leg. A cast model was made of my leg and foot, on this model layers of carbon fiber were laid. The cast model is shown in Figure 17.



Figure 17, the cast model of my right lower leg.

The layers of carbon fiber are then impregnated with epoxy raisin. The epoxy raisin is inseminated during vacuum condition. In Figure 18 a picture of the NSO is made just after the prototype was inseminated with epoxy.



Figure 18. At the left side the NSO was just inseminated with raisin. At the right side the finalizing begins, the shin part of the NSO is separated from the cast mold.

After 1 hour the epoxy is hardened and the prototype is separated from the mold. The excessive material is cut out and the NSO is sanded for a good finish. The bandages are put on and in the last stage some minor sanding is done to make sure the NSO matches my foot.

2.3 Experiment

Validate design

The design is successfully transformed into a prototype and validation is needed. The orthosis is measured in terms of weight and volume. The torque-angle relation is measured of the prototype NSO.

Case study

Since walkability is a goal for this project it is checked in a case study. In this case study I get tested on a treadmill. In 30 seconds a walking exercise take place at my preferable walking speed. During this exercise the EMG(Electromyography)-activity for both legs are measured for four muscle groups: Tibialis Anterior, Soleus, Gastrocnemius Medialis en Gastrocnemius Lateralis. The same test is done for six different conditions:

- In the first condition is the subject performs a walking test without NSO.
- In the second test the subject performs a walking test with the NSO but without any compensational torque.
- In the last four tests the subject wears the NSO with a compensational torque but with different levels of compensation. The third test with the lowest compensation and for the sixth test the compensational torque is highest.

3. Results

3.1 Model

The theoretical model that simulates the torque-angle relation for different configuration of the magnet is the first result of my thesis. The Matlab model includes the force distance relation of the magnet and is included in Appendix A. In this model the input is the amount of magnets at chosen lengths to the pivot point. The model output is the torque-angle relation for the chosen configuration of magnets. The output exists of the energy efficiency: $\frac{\textit{Work done by magnet}}{\textit{energy available in magnet}}.$

3.2 Prototype

The resulting prototype is shown in Figure 19. The outer dimensions are equal to $460 \ mm \times 190 \ mm \times 290 \ mm$. The total mass of the prototype is 1.296 kg.



Figure 19a: right side of the Negative Stiffness Orthosis.



Figure 19b: side view from left of the Negative Stiffness Orthosis.



Figure 19c, Front view of the Negative Stiffness Orthosis.

The prototype was fabricated to fit the shape of my leg and foot. The NSO matches my leg and foot perfectly, the NSO does not cause an inconvenient experience in terms of comfort during use.

The torque-angle relation of the NSO was measured. The measured torque-angle relation is showed in Figure 20 and compared to the NAS2 torque-angle relation.

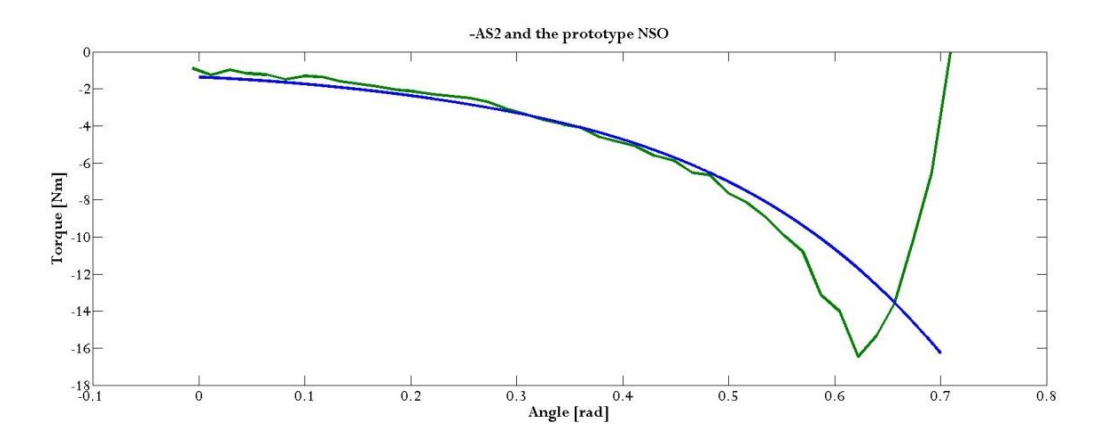


Figure 20: NAS2(blue line) and the torque measurement of the prototype (green line). The prototype has magnets with the Length PP1= 15 mm, Length PP2= 15 mm, Length PP3 = 42 mm and Length PP4 = 42 .

The measured torque-angle relation off the NSO prototype is measured in Figure 20.

3.3 Case study

Walkability

The prototype NSO is tested during walking conditions. I performed a 30 second walking exercise on a treadmill with a speed of 3.8 km per hour for 6 different conditions.

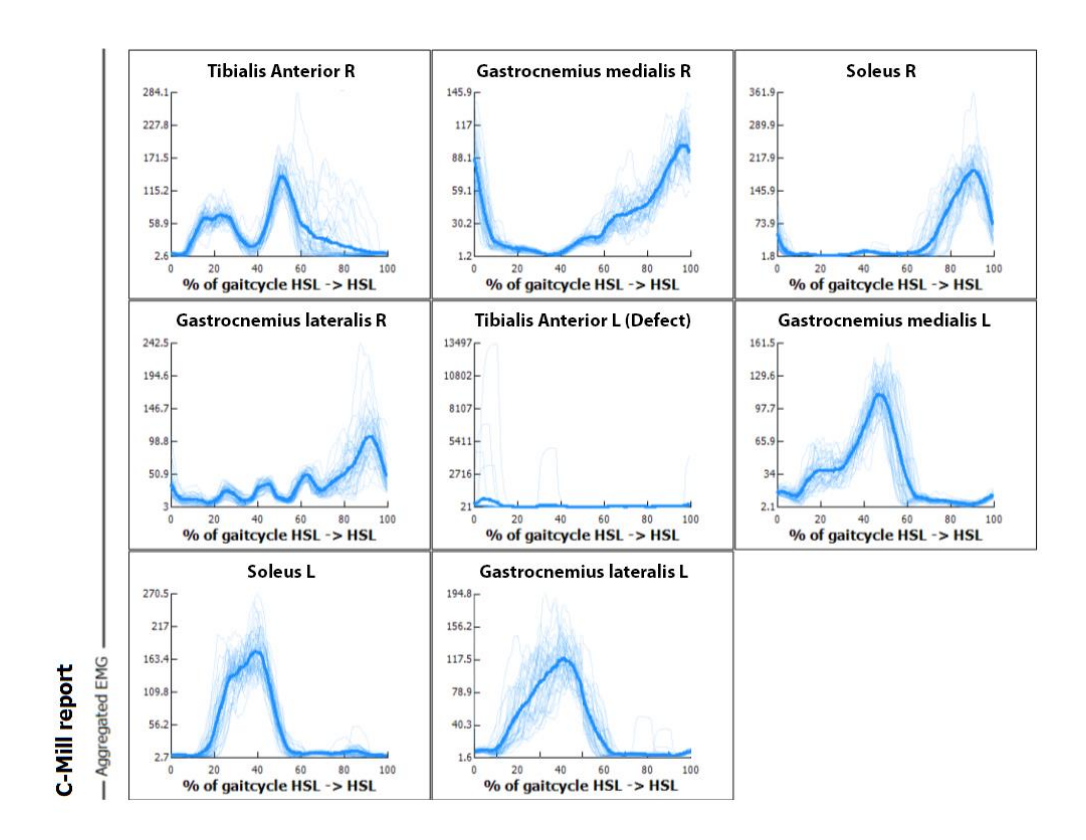


Figure 21, EMG-activity for walking test without NSO. The aggregated EMG-activity for the left (L) and right (R) leg. For each muscle group the EMG-activity is shown on the Y-axis, the X-axis represent the percentage of a walking step. At 0% Heel Strike with Left (HSL) leg occurs and at 100% HSL occurs again.

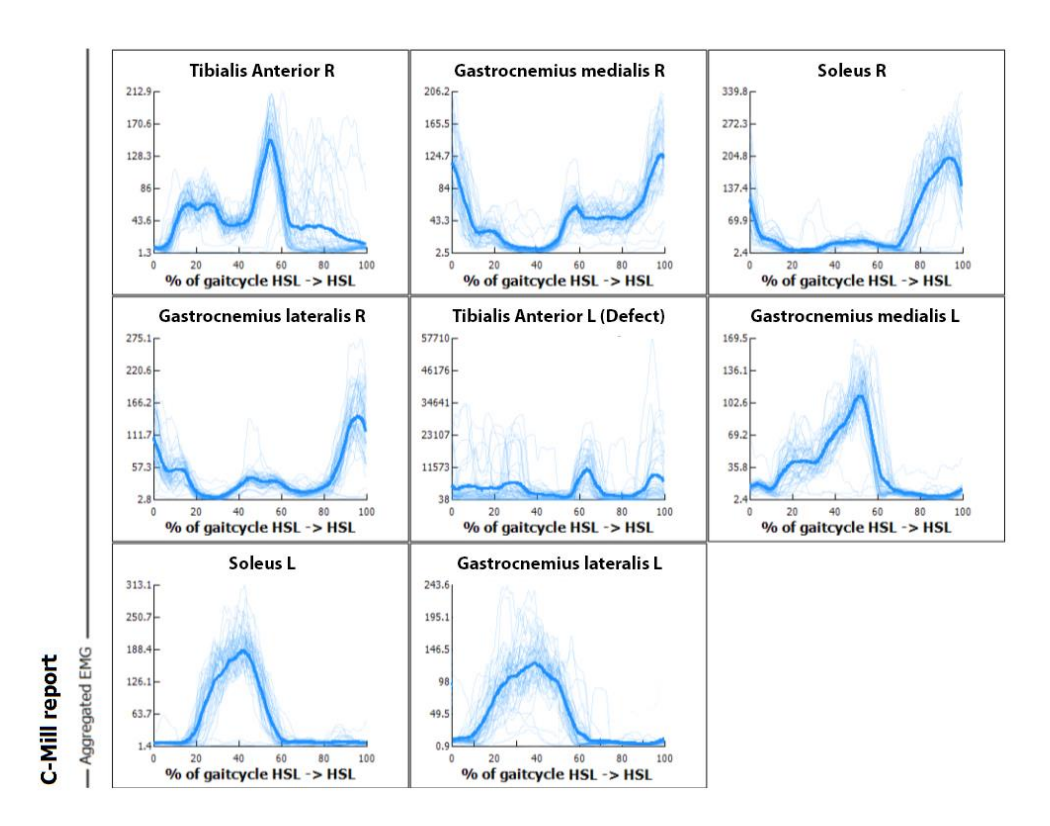


Figure 22, EMG-activity for walking test with NSO without magnets. The aggregated EMG-activity for the left (L) and right (R) leg. For each muscle group the EMG-activity is shown on the Y-axis, the X-axis represent the percentage of a walking step. At 0% Heel Strike with Left (HSL) leg occurs and at 100% HSL occurs again.

To validate the walkability of the NSO two walking conditions were compared. The first condition was a walking test without NSO and the second condition was a walking test with NSO without compensation (zero magnets). Figure 21 and 22 show the average normalized EMG-activity for the Tibialis Anterior, Soleus, Gastrocnemius Medialis and Gastrocnemius Lateralis for the left and the right leg. The EMG-activity for the test with NSO is higher than the EMG-activity for the test without NSO.

Tibialis Anterior EMG-activity

For walking tests 3 to 6 the compensation by the NSO was increased, in test 6 the compensation was the highest, with the torque-angle relation as plotted in Figure 20.

The EMG signal of the Tibialis Anterior muscle is measured during the 30-second walking exercise. In Appendix B the EMG signals for all muscle groups are plotted. Figure 23 shows the EMG-activity of the Tibialis Anterior for all 6 tests.

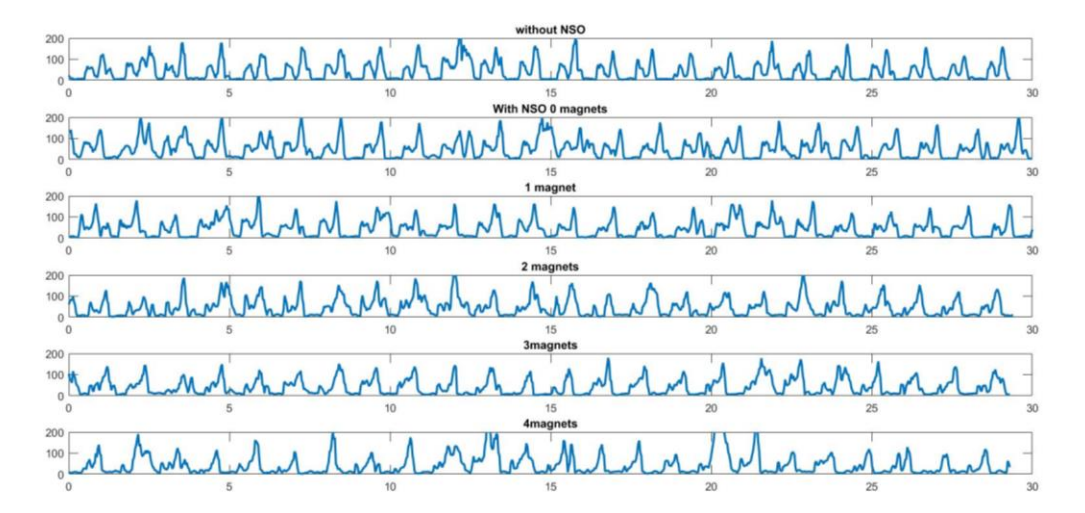


Figure 23: 6 tests show an EMG-signal of the Tibialis Anterior. The x-axis shows the time the y-axis shows the aggregated EMG-activity.

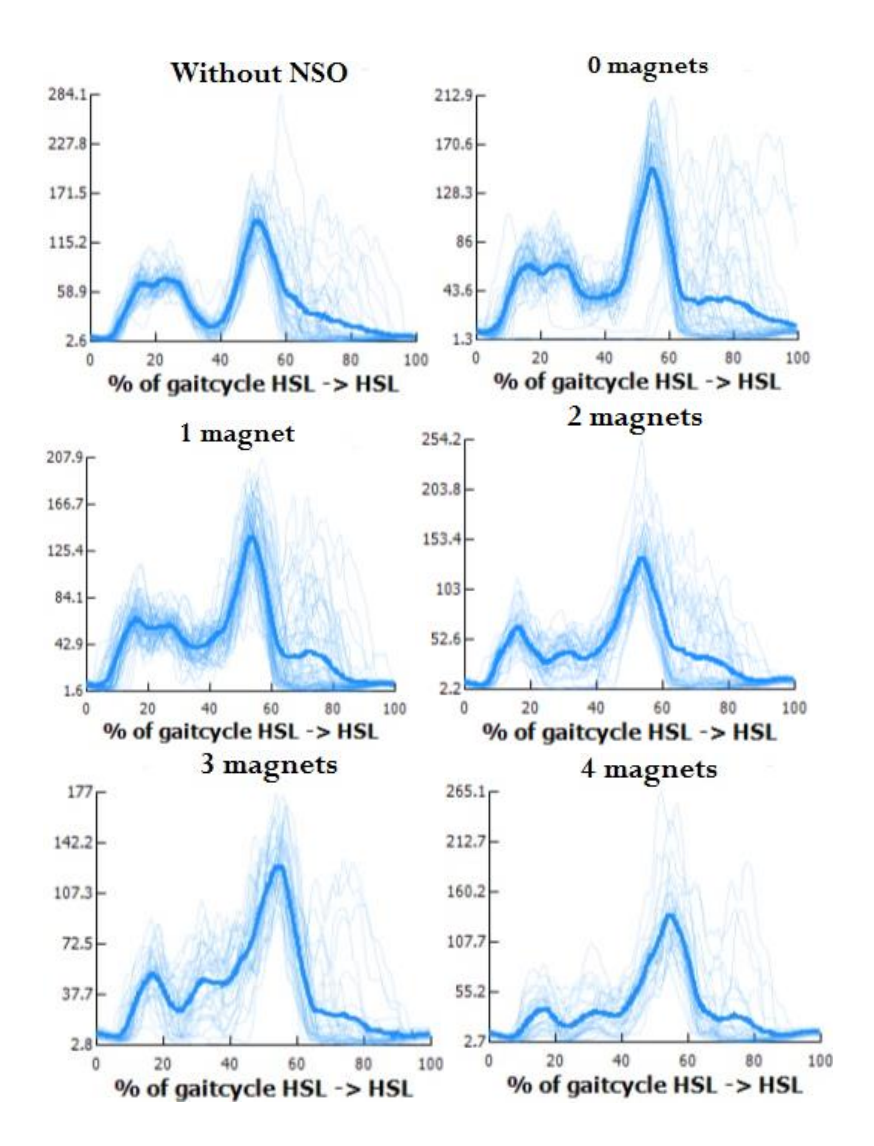


Figure 24: The aggregated EMG-activity for the six tests is plotted. For each muscle group the EMG-activity is shown on the Y-axis, the X-axis represent the percentage of a walking step. At 0% Heel Strike with Left (HSL) leg occurs and at 100% HSL occurs again. The thick blue line is the avarage EMG-activity.

In the walking test instable steps results in outliers in the measurement of the EMG-activity. Figure 23 shows an example of an instable step at around 20 seconds for the test with 4 magnets. The video recording shows that indeed at this point an unstable step was made. Figure 24 shows the EMG-activity for the Tibialis Anterior against the percentage of gait cycle.

Figure 24 shows two peaks in EMG-activity, the first peak at 20% of the gait cycle corresponds to the EMG-activity of the Tibialis Anterior to lift the foot during swing phase. The second peak is at 50% of the gait cycle and corresponds to the contraction of the Tibialis Anterior during heel strike. The EMG-activity for the two peaks is summarized in the table 2. The average EMG-activity is calculated by using the data shown in Figure 23, outliers are excluded.

Table 2: Average EMG-activity in Tibialis Anterior for the Heel Strike and the Swing Phase.

compensation	Heel	Swing		
	strike	Phase		
0 magnets	170	79		
1 magnet	152	71		
2 magnets	148	66		
3 magnets	137	52		
4 magnets	138	41		

Table 2 shows that there is a difference in effect on EMG-activity during swing phase and heel strike. During the swing phase the EMG-activity is the most influenced: going from 79 in the situation without compensation to an activity of 41 with maximum compensation of 4 magnets. For the Heel Strike the EMG-activity goes from 170 with no compensation to 137 with a compensation of 3 magnets.

4. Discussion

For this study a Negative Stiffness Orthosis was built to compensate increased passive ankle stiffness. The magnetic neodymium was used to realize the NAS2 torque-angle relation. A computer model was made to realize a theoretical concept for the NSO. The effect of different levels of stiffness compensation has been tested on an able-bodied subject during a walking exercise.

4.1 Model

The mechanism that realizes the negative torque-angle relation consists of multiple magnets attached on two beams connected at one pivot point. The working principle is able to change the torque-angle relation in terms of shape and amplitude choosing the configuration of magnets on the beam. The idea has been verified by a theoretical model Appendix A. The model confirms that the torque-angle relation can be tuned by placing the magnets either closer or further from the pivot point, series placement. To increase the amplitude, multiple magnets can be placed at the same length to the pivot point, parallel placement. The distance from the magnet to the pivot point has an effect on energy efficiency. When magnets are placed relatively close to the pivot point the magnets are not separated up to their full magnetic force field for the maximum angle. Therefore, not all potential energy is transformed into work, energy efficiency is lower. Energy efficiency can be seen as a measurement for performance of the configuration of magnets.

Energy efficiency

The goal for the model was to find the configuration with the highest energy efficiency while reaching the NAS2 torque-angle profile. The search for the ideal configuration was done by hand with the knowledge of the effect of placing magnets. An energy efficiency of 88% was achieved. A Computational optimization for the magnet configuration is expected to increase the energy efficiency with a few percent.

Patient specific NSO

For the model in Appendix A the torque-angle relation was derived from the average patient characteristic and taken as the exponential function AS2. It would be ideal to design a compensating torque-angle relation specifically for individual patients. The realization of the NAS2 torque-angle relation implies that torque-angle relations lower than NAS2 can be realized. In this case AS2 was used as torque-angle relation, but various shapes of torque-angle relation are needed for various patients.

The mechanism is able to realize different shapes of torque-angle relation and it is a promising mechanism to compensate for the patient-specific torque-angle relation.

Assumptions

Figure 20 shows the torque-angle relation of the prototype that the model does not predict the torque-angle relation correctly. Figure 20 shows the configuration with magnets respectively on Length PP1= 15 mm, Length PP2= 15 mm, Length PP3 = 42 mm and Length PP4 = 42. The measured work delivered by the magnets is 3.76 joule. The model predicted an estimated delivered work of 2.89 Joule. The model underestimates the attraction forces.

In the model two assumptions were made. The first assumption was that the poles of the magnets were always facing each other, whereas in the prototype the magnets face each other at an angle. This assumption overestimates the magnetic forces in the model.

The second assumption was that only the attraction force between a pair of magnets existed. All magnets with opposite poles exert an attraction force on each other which results in an additional attraction force. The second assumption underestimates the magnetic forces in the model. This assumption accounts for the biggest deviation of the predicted torque-angle relation. The underestimation of the attraction forces resulted in a magnetic configuration lighter than expected.

4.2 Prototype

The weight and volume were key parameters for the realization of a walkable NSO. The weight of the NSO is 1290 gram and the size is $460 \, mm \times 190 \, mm \times 290 \, mm$. A similar sized AFO produced by Noppe Orthopedics weighs around 800 grams. The two arms with the magnets attached are responsible for the higher weight of the NSO. The NSO to subject interaction is comparable to AFOs produced by Noppe Orthopedics.

Table 3: The values for the NSOs are deducted from table 1 as presented in Shorter [17]. The properties of the TU Delft NSO are added to table 3.

	Weig ht	Resistiv e or Assistiv e	Active Element	Maxim um applied Force	Advantages	Disadvanta ges	Performa nce metrics	Experimen tal Evaluation	Results
DACS AFO [10]	0.3 kg	Resistive	Mechanic al Spring	17 Nm (per 10 deg of rotation)	Compact, light weight, untethered, interchangeable springs for patient specific assistance	Constant resistive force impedes motion	Gait speed and qualitative visual inspection of gait	Five Hemiplegic subjects walked with DACS, posterior leaf spring, and metal-leather AFO	DACS AFO users had faster and smoother gait
Univer sity of Illinois AFO [18]	1 kg	Resistive	Locking CAM	?	Variable motion control untethered and the energy to actuate the locking mechanism harvested during gait	Bulky AFO structure complicated locking system	Joint angle kinematics , pneumatic line pressure	Single healthy subject	Joint angle data demonstrated proper foot motion and pneumatic pressure data showed correct locking sequence during gait
Kanaga wa Rehabi litatio n center AFO [19]	0.4 kg	Resistive	Oil damper	5-14 Nm (at 10 degrees of plantar flexion)	Variable motion control, untethered, light weight and the resistive force is easily adjustable	Resistive force is the same during initial stance and swing	Time, Distance and kinematic parameter s	Two hemiplegic patients walked with oil damper and conventional AFO	No significant functional difference between the AFOs. Oil damper's largest advantage was ease of adjustability
Okaya ma Univer sity AFO [20]	0.86 kg	Assistive	Pneumati c Actuator	2 Nm	Variable motion control, untethered, energy to actuate the active element is harvested during gait	Has a bulky AFO structure and only generates small assistive torques	EMG	Single healthy individual	Decrease in EMG signal during trials indicates supplemental assistance
TU Delft NSO Pim Brandj es	1.3 kg	Assistive, Negative stiffness	Magnets	16 Nm	Adjustable torque-angle relation, untethered, possibly improving RoM	Has a bulky AFO structure. Magnet attracts metal.	EMG	Single healthy individual	Decrease in EMG-activity in TA during walking tests.
TU Delft NSO Freek Verbak el [13]	3.5 kg	Assistive, Negative stifness	Mechanic al spring	7.5 Nm	Adjustable torque-angle relation untethered, possibly improving RoM	Not wearable while walking. Bulky and heavy design	EMG	10 subjects	Increase in dorsiflexion RoM in sedentary position

Shorter [17] presented a comparison between novel passive AFOs designs. There are two different types of AFOs classified in Table 3, respectively resistive and assistive AFOs. The NSO is a novel principle and classified as an assistive Orthosis. The assistive AFO from Okayama University [20] in Table 3 exerts a positive stiffness while the NSO exerts a negative stiffness. The NSO is able to generate a torque with a maximum of 16 Nm were the assistive AFO by Okayama University [20] generates a maximum torque of 2 Nm. The previous version of the TU Delft NSO by Verbakel [12], weighs 3.5 kg with a maximal torque of 7.5 Nm. For the Orthoses classified as assistive the NSO is able to generate the highest torque; more than two times as high as the previous prototype and eight times as high as the AFO from the Okayama University. The extra weight for the NSO compared to the AFO from Okayama University can be explained by the ability to generate an 8 times higher torque.

The AFOs designs of University of Illinois [18] and from the Kanagawa Rehabilitation Center [10] use harvested energy to "lock" the orthoses during swing phase, with weights respectively 1 kg and 0.4 kg. They both aim to achieve toe clearance during swing phase and free ankle motion during stance phase. The DACS AFO[5] is a passive positive stiffness Orthosis. If the NSO is compared to the resistive orthoses in terms of weight the NSO is heavier than these Orthoses. The resistive Orthoses are positive stiffness systems while the NSO is a negative stiffness system therefore a weight difference is expected. Before a comparison for maximum torque can be made between the orthoses a remark has to be made. In Table 3 Shorter[17] labeled a column with the property 'Maximum applied Force'. For passive orthoses the word 'applied force' is not accurate because no torque is generated by the orthoses. Because the orthoses are 'locked' the maximum torque only occurs for deformation of the AFO, a better definition would be 'resistive force'. The NSO applies a torque where the AFOs resist a torque therefore a comparison is not possible. The function of the resistive AFOs is different and results in a lighter and less bulky solution, but the RoM of the patient decreases. Whereas the NSO aims to increase Range of Motion.

It can be concluded that, in terms of weight and maximum torque, the NSO performs better than other assistive AFOs. Compared to resistive AFOs, the NSO is a bit heavier than resistive AFOs. However, resistive AFOs result in a decreased RoM and simply 'lock' the foot of the patient, whereas the the NSO aims to increase Range of Motion, which is vital in improving gait efficiency.

Fabrication

The fabrication of the NSO was done professionally with comparable materials used as in regular AFO's. The lack of experience in building this first prototype was the cause of unnecessary use of material which made this prototype heavier than needed. There is not much room for weight reduction by choosing lighter or better materials.

Material stiffness

Figure 20 shows the peak torque has a 0.08 radians offset from the desired NAS2 torque-angle relation. The offset is due to the deformation of material in the prototype, in other words the prototype is too compliant. The magnets almost touch each other at 0.7 rad. If the NSO is moved towards 0 rad the NSO deforms before the magnets start to separate. At 0.62 rad the magnets start to separate, at this point the peak torque of the NSO occurs. This problem can be solved for the next generation NSO by using more material to increase stiffness at the shoe size of the NSO.

4.3 Case study

Walkability

Figure 21 and 22 show the average normalized EMG-activity for the Tibialis Anterior, Soleus, Gastrocnemius Medialis and Gastrocnemius Lateralis for the left and the right leg. The EMG-activity for the condition with NSO is higher than the EMG-activity of the situation without NSO. The increase in EMG-activity in the right leg can be related to increased muscle force. The increase in muscle force is needed to compensate for the extra weight of the NSO carried by the right leg.

Effect

The aim of the comparison is to gain insight in the behavior of the EMG-activity of the Tibialis Anterior during walking conditions while a negative torque-angle is applied. Table 2 shows that there is a difference in effect on EMG-activity during swing phase and heel strike. During the swing phase the EMG-activity is the most influenced: going from 79 in the situation without compensation to an activity of 41 with maximum compensation of 4 magnets. A reduction in EMG-activity can be explained by torque generated by the NSO in dorsiflexion direction. The needed torque to lift the foot is less, resulting in less force needed by the TA. For the Heel Strike the EMG-activity goes from 170 with no compensation to a minimum of 137 with a compensation of 3 magnets. The effect of the compensating torque-angle relation is less for Heel Strike.

4.4 Recommendations

Suggestions can be made for future research and development of the NSO. The model for the torque-angle relation should be extended in order to be able to predict the torque-angle relation more accurate. I suggest that for the future model all the attraction forces should be described, this will result in accurate estimation of the attraction forces. In this cas the measured torque-angle relation of the patient can be accuratly translated into a design with according configuration of magnets.

For the prototype emphasis should be put on creating a stiffer orthosis. The configuration of the magnets should be adjustable like in this prototype, so that various torque-angle relations can be achieved.

For future research the effect of a torque-angle relation that compensate their passive stiffness in the ankle-joint should be investigated. The study must investigate two factors. The first factor is Range of Motion, will the NSO contribute to an increase in RoM? The second factor should focus on the effect of the NSO on walking gait. What effect does the compensation of the passive stiffness in the ankle joint has on the gait of a patient?

5. Conclusion

In this study a Negative Stiffness Orthosis(NSO) was designed, build and evaluated. The Orthosis is based on a novel approach to compensate passive stiffness in the ankle joint for patients suffering from drop foot. Magnetic neodymium was used to generate a compensating torque-angle relation for patients with a passive ankle stiffness classified as Ashworth 2. A model was introduced and predicted a torque-angel relation for a given configuration of neodymium magnets. The configuration of the magnets in the NSO can be changed to shape the torque-angle relation of the NSO, in order to create a patients' specific torque-angle relation.

The experiments show that the walkability of the NSO was sufficient. The EMG-activity in the Tibialis Anterior decreases during swing phase and heel strike for an increasing compensational torque-angle relation.

The effect on the Range of Motion for patients has not been researched, nevertheless the reduced EMG-activity in the Tibialis Anterior suggest that an increase in RoM can be expected.

This study suggests that this NSO potentially benefit patients with increased passive stiffness in the ankle joint during walking.

6. Reference

- [1] S. A. Ross and J. R. Engsberg, "Relationships between spasticity, strength, gait, and the gmfm-66 in persons with spastic diplegia cerebral palsy," *Archives of Physical Medicine and Rehabilitation*, vol. 88, no. 9, pp. 1114 1120, 2007.
- [2] L. Ballaz, S. Plamondon, and M. Lemay, "Ankle range of motion is key to gait efficiency in adolescents with cerebral palsy," *Clinical Biomechanics*, vol. 25, no. 9, pp. 944 948, 2010.
- [3] J. Bregman, "The optimal ankle foot orthosis," Muscle Nerve, 2011.
- [4] J. Burridge, D. Wood, P. Taylor, and D. McLellan, "Indices to describe different muscle activation patterns, identified during treadmill walking, in people with spastic drop-foot," *Medical Engineering amp; Physics*, vol. 23, no. 6, pp. 427 434, 2001.
- [5] Erwin de Vlugt, Jurriaan H. de Groot, Wessel H.J. Wisman, and Carel G.M. Meskers. "Clonus is explained from increased reflex gain and enlarged tissueviscoelasticity." *Journal of Biomechanics*, 45(1):148 { 155, 2012.}
- [6] www.gipdatabank.nl, het Genees- en hulpmiddelen Informatie Project (GIP), Diemen: College voor zorgverzekeringen 2014
- [7] F. Verbakel, "Stiffness compensation in Ankle-Foot Orthosis," 2012.
- [8] K. A. Shorter, J. Xia, E. T. Hsiao-wecksler, and W. K. Durfee, "Technologies for Powered Ankle-Foot Orthotic Systems: Possibilities and Challenges."
- [9] J. Perry, "Gait Analysis: Normal and Pathological Function." Thorofare, 780 NJ: SLACK, Inc., 1992.
- [10] Yamamoto, S., et al, "Development of an Ankle-Foot Orthosis with Dorsiflexion Assist, Part 2: Structure and Evaluation." *Journal of Prosthetics and Orthotics*, 1999. 11(2): p. 24-27.
- [11] H. Teyssedre and G. Lefort, "Dynamic Orthesis," Eur. Patent Office, France, pp. 1–9, 2005.
- [12] F. Verbakel, "Design and evaluation of a stiffness compensating ankle-foot orthosis," 2013.
- [13] L. Derks, "The effects of passive stiffness compensation, by negativ stiffness, on active RoM and controllability of the ankle joint." 2012
- [14] P.E.M. Brandjes, "Energy storage in Negative Stiffness Orthosis, Quantitative comparison for specific energy and energy density for energy storage systems" 2015
- [15] http://www.supermagnete.nl/eng/disc-magnets-neodymium-large/disc-magnet-diameter-20mm-height-10mm-neodymium-n42-nickel-plated_S-20-10-N?img=1
- [16] http://www.kjmagnetics.com/faq.asp#lose K&J Magnets

- [17] Shorter, K.A., et al, "Technologies for Powered Ankle-Foot Orthotic Systems: Possibilities and Challenges." *IEEE Transactions on Mechatronics*, 2011.
- [18] R. Chin, E. T. Hsiao-Wecksler, E. Loth, G. Kogler, S. Manwaring, K. A. Shorter, S.N. Tyson, and J.N. Gilmer, "A pneumatic power harvesting anklefoot orthosis to prevent foot-drop," *J. NeuroEng. Rehabil.*, vol. 6, no. 19, Jun. 16, 2009.
- [19] O. Yokoyama, H. Sashika, A. Hagiwara, S. Yamamoto, and T. Yasui, "Kinematic effects on gait of a newly designed ankle-foot orthosis with oil damper resistance: A case series of 2 patients with hemiplegia," *Archives Phys. Med. Rehabil.*, vol. 86, pp. 162–166, 2005.
- [20] M. Takaiwa and T. Noritsugu, "Development of pneumatic walking support shoes using potential energy of human," in *Proc.7thJpn.FuildPower System Int. Symp. Fluid Power*, Toyama, Japan, 2008, pp. 781–786.

7. Appendix A

```
close all
%hoek van
             maximale plantarflextion(0) naar maximale
dorsiflexion(0.7)
hoek=0:0.0001:0.7;
% %afstand tot draaipunt magneet 1
% lengtearm1=0.032;
% %afstand tot draaipunt magneet 2
% lengtearm2= 0.021;
% %afstand tot draaipunt magneet 3
% lengtearm3= 0.027;
%afstand tot draaipunt magneet 1
lengtearm1=0.020;
%afstand tot draaipunt magneet 2
lengtearm2= 0.018;
%afstand tot draaipunt magneet 3
lengtearm3= 0.028;
%afstand tot draaipunt magneet 4
lengtearm4= 0.042;
%afstand tot draaipunt magneet 5
lengtearm5= 0.026;
%magneet 1 beweging
fctr1= sin(0.7/2)*lengtearm1; %maximale afstand
x1= 0.04-2*fctr1+2*(sin(hoek/2).*lengtearm1); %afstand tussen
magneten
x1 = max(0, x1);
%magneet 2 beweging
fctr2= sin(0.7/2)*lengtearm2;
x2=0.04-2*fctr2+2*(sin(hoek/2).*lengtearm2);
x2 = max(0, x2);
%magneet 3 beweging
fctr3= sin(0.7/2)*lengtearm3;
x3 = 0.04 - 2 \cdot fctr3 + 2 \cdot (sin(hoek/2). \cdot lengtearm3);
x3 = max(0,x3);
%magneet 4 beweging
fctr4= sin(0.7/2)*lengtearm4;
x4 = 0.04 - 2 \cdot fctr4 + 2 \cdot (sin(hoek/2). \cdot lengtearm4);
x4 = max(0,x4);
%magneet 5 beweging
fctr5= sin(0.7/2)*lengtearm5;
x5 = 0.04 - 2 \cdot fctr5 + 2 \cdot (sin(hoek/2). \cdot lengtearm5);
x5 = max(0, x5);
%grafiek afstand tussen magneten op y as tov hoek op de x-as
% plot(hoek,x1,hoek,x2,hoek,x3)
% title('hoek-afstandmagneten')
% ylabel('afstandtussenmagneten')
% xlabel('hoek')
_____
8______
_____
%benadering van kracht/lengte met x als afstand tussen de
magneten voor
```

```
%0.04 raken de magneten elkaar net%Coefficients
  ap1 = 3.6125e + 18;
  ap2 = -6.4421e+17;
  ap3 = 4.8791e+16;
  ap4 = -2.038e+15;
  ap5 = 5.1099e+13;
  ap6 = -7.8355e+11;
 ap7 = 7.173e + 09;
  ap8 = -3.5982e+07;
  ap9 = 87890;
  ap10 = 75.604;
 ap11 = 1.6542;
 f1 = -1*(ap1*x1.^10 + ap2*x1.^9 + ap3*x1.^8 + ap4*x1.^7 +
ap5*x1.^6 + ap6*x1.^5 +
                                    ap7*x1.^4 + ap8*x1.^3 +
ap9*x1.^2 + ap10*x1 + ap11) ; %magneet 1
f2 = -1*(ap1*x2.^10 + ap2*x2.^9 + ap3*x2.^8 + ap4*x2.^7 +
ap5*x2.^6 + ap6*x2.^5 +
                                    ap7*x2.^4 + ap8*x2.^3 +
ap9*x2.^2 + ap10*x2 + ap11 ); %magneet 2
f3 = -1*(ap1*x3.^10 + ap2*x3.^9 + ap3*x3.^8 + ap4*x3.^7 +
ap5*x3.^6 + ap6*x3.^5 +
                                    ap7*x3.^4 + ap8*x3.^3 +
ap9*x3.^2 + ap10*x3 + ap11 ); %magneet 3 f4 = -1*(ap1*x4.^10 + ap2*x4.^9 + ap3*x4.^8 + ap4*x4.^7 +
ap5*x4.^6 + ap6*x4.^5 +
                                    ap7*x4.^4 + ap8*x4.^3 +
ap9*x4.^2 + ap10*x4 + ap11 ); %magneet 4 f5 = -1*(ap1*x5.^10 + ap2*x5.^9 + ap3*x5.^8 + ap4*x5.^7 +
ap5*x5.^6 + ap6*x5.^5 +
                                    ap7*x5.^4 + ap8*x5.^3 +
ap9*x5.^2 + ap10*x5 + ap11 ); %magneet 5
% f1 = (ap1*x1.^10 + ap2*x1.^9 + ap3*x1.^8 + ap4*x1.^7 + ap5*x1.^6 + ap6*x1.^5 + ap7*x1.^4 + ap8*x1.^3 +
ap9*x1.^2 + ap10*x1 + ap11); %magneet 1
% f2 = (ap1*x2.^10 + ap2*x2.^9 + ap3*x2.^8 + ap4*x2.^7 +
ap5*x2.^6 + ap6*x2.^5 +
                                    ap7*x2.^4 + ap8*x2.^3 +
ap9*x2.^2 + ap10*x2 + ap11); %magneet 2
% f3 = (ap1*x3.^10 + ap2*x3.^9 + ap3*x3.^8 + ap4*x3.^7 +
ap5*x3.^6 + ap6*x3.^5 +
                                    ap7*x3.^4 + ap8*x3.^3 +
ap9*x3.^2 + ap10*x3 + ap11); %magneet 3
f4 = (ap1*x4.^10 + ap2*x4.^9 + ap3*x4.^8 + ap4*x4.^7 +
ap5*x4.^6 + ap6*x4.^5 +
                                    ap7*x4.^4 + ap8*x4.^3 +
ap9*x4.^2 + ap10*x4 + ap11); %magneet 4
f5 = (ap1*x5.^10 + ap2*x5.^9 + ap3*x5.^8 + ap4*x5.^7 +
ap5*x5.^6 + ap6*x5.^5 +
                                    ap7*x5.^4 + ap8*x5.^3 +
ap9*x5.^2 + ap10*x5 + ap11 ); %magneet 5
%2 magneten van 0 tot 0.4 naar elkaar gebracht
x7=0:0.0001:0.04;
f7 = -1.*(ap1*x7.^10 + ap2*x7.^9 + ap3*x7.^8 + ap4*x7.^7 +
ap5*x7.^6 + ap6*x7.^5 +
                                    ap7*x7.^4 + ap8*x7.^3 +
ap9*x7.^2 + ap10*x7 + ap11); %magneet 4
%kracht tot afstand tussen de magneten
figure
plot(x1, f1, x7, f7, ':')
title('kracht-lengte')
ylabel('kracht [n]')
xlabel('lengte [m]')
% figure
% plot(x2,f2,x4,f4,':')
```

```
% title('kracht-lengte')
% ylabel('kracht [n]')
% xlabel('lengte [m]')
% figure
% plot(x3,f3,x4,f4,':')
% title('kracht-lengte')
% ylabel('kracht [n]')
% xlabel('lengte [m]')
%-----
_____
8-----
%voor het berekenen van torque moet ook nog de functie van de
arm worden
%gedefinieerd als functie van hoek
%momentarm van magneet op plek 1
momentarm = (cos((0.7-hoek)/2))*lengtearm1;
%momentarm van magneet op plek 2
momentarm2 = (cos((0.7-hoek)/2))*lengtearm2;
%momentarm van magneet op plek 3
momentarm3 = (cos((0.7-hoek)/2))*lengtearm3;
%momentarm van magneet op plek 4
momentarm4 = (cos((0.7-hoek)/2))*lengtearm4;
%momentarm van magneet op plek 5
momentarm5 = (cos((0.7-hoek)/2))*lengtearm5;
%hoek tegen momentarm voor plek 1 en plek 2
figure
plot (hoek, momentarm, hoek, momentarm2, hoek, momentarm3, hoek, moment
arm4, hoek, momentarm5)
title('momentarm')
xlabel('Angle [rad]')
ylabel('kracht [n]')
                ._____
%curve patient
% c1=0.138;
% c2=4.85;
% c3=1.25-0.5;
% x=0:0.0001:0.70;
% AS3=1*(1.5+c1*exp((x+c3)*c2-2.2));
%AS2
 zp1 = 62.5;
 zp2 = -29.672;
 zp3 = 17.405;
 zp4 = 2.2123;
 zp5 = 1.372;
AS2 = -1*(zp1*hoek.^4 + zp2*hoek.^3 +
                                      zp3*hoek.^2 +
zp4*hoek + zp5);
%AS3
p1 = 102.27;
```

```
p2 = -79.04;
  p3 = 41.174;
  p4 = -0.89033;
  p5 = 1.6242;
AS3 = p1*hoek.^4 + p2*hoek.^3 +
                                         p3*hoek.^2 + p4*hoek+
p5 ;
%Moment
%moment door magneet op plek 1
aantalmagneet1 = 1; %aantal magneten op plek 1
M1= aantalmagneet1*f1.*momentarm;
%moment door magneet op plek 2
aantalmagneet2= 1;
M2= aantalmagneet2*f2.*momentarm2;
TWM2 = 2.*M2;
%moment door magneet op plek 3
aantalmagneet3= 1;
M3= aantalmagneet3*f3.*momentarm3;
TWM3 = 2.*M3;
%moment door magneet op plek 3
aantalmagneet4= 1;
M4= aantalmagneet4*f4.*momentarm4;
TWM4 = 2.*M4;
%moment door magneet op plek 5
aantalmagneet5= 1;
M5= aantalmagneet5*f5.*momentarm5;
TWM5 = 2.*M5;
%totaal moment door magneten
Mmag = M1 + M2 + M3 + M4 + M5;
% TWM1= 2.*M1;
% DRM1= 3.*M1;
% VIM1= 4.*M1;
% VFM1= 5.*M1;
% % ZEM1= 6.*M;
% ZEM1OP= M1+M1+M1+M1+M1;
% ZVM1= 7.*M1;
% ACM1= 8.*M1;
% NEM1= 9.*M1;
% TIM1= 10.*M1;
% figure
% plot(hoek, AS2, hoek, M1, hoek, TWM1, hoek, DRM1, hoek, VIM1, hoek,
VFM1, hoek, ZEM1OP, hoek, ZVM1, hoek, ACM1, hoek, NEM1, hoek, TIM1)
% title('-AS2, and from 1 to 10 magnets on Length PP= 0.1
meter')
% xlabel('Angle [rad]')
% ylabel('Torque [Nm]')
%hoek tegenovermoment voor magneten op plek 1 en op plek2 en op
plek 3 en allebei
figure
plot (hoek, M1, hoek, M2, hoek, M3, hoek, M4, hoek, M5, hoek, Mmag)
title('moment magneten')
xlabel('Angle [rad]')
ylabel('Torque [Nm]')
```

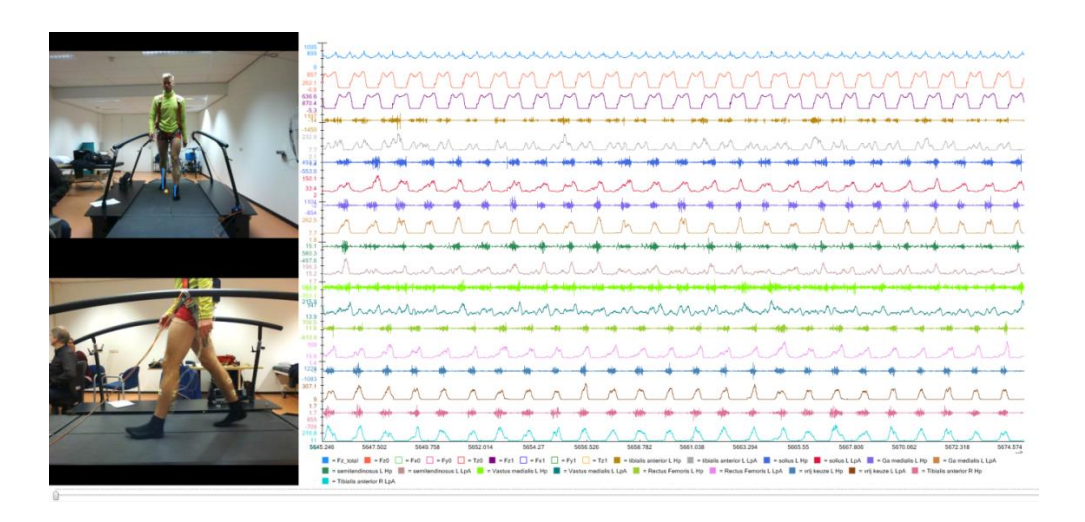
```
% %-----MetingNSO-----
%Meting 1
radians1=
                       (([61,62,63,64,65,66,67,68,69,70,71,72,
73,74,75,76,77,78,79,80,81,82,83,84,85,86,87,88,89,90,91,92,93,
94,95,96,97,98,99,100] )-90)*0.0174532925199 +0.5;
torque1
0.00980665002864*[99,101,105,118,113,148,148,165,170,180,150,20]
210, 225, 236, 230, 220, 280, 280, 280, 250, 330, 260, 380, 400, 450, 470, 545
,530,595,600,630,720,960,1060,1280,1520,1360,1520,860];
%meting 2
radians2=
1,82,83,84,85,86,87,88,89,90,91,92,93,94,95,96,97,98,99,100,101
,102] -90) *0.0174532925199 +0.5;
torque2
0.00980665002864*[91,129,100,119,126,152,134,139,164,178,192,20]
9,218,234,244,255,276,315,346,376,398,418,470,496,523,572,598,6
64,679,780,832,912,1013,1100,1342,1430,1680,1564,1380,1033,660,
0];
figure
plot(radians1, torque1)
figure
plot(radians2, torque2, hoek, AS2)
title('-AS2 and the prototype NSO')
xlabel('Angle [rad]')
ylabel('Torque [Nm]')
%_____
figure
plot(hoek,MT)
title(' resultante')
xlabel('Angle [rad]')
ylabel('Torque [Nm]')
%%Moment resultante
MT= AS2-Mmag;
figure
plot(hoek, AS2, hoek, Mmag, ':', hoek, MT)
title('moment magneten en patient en resultante')
xlabel('Angle [rad]')
ylabel('Torque [Nm]')
%StijfheidPatient= T./hoek;
%StijfheidMmag= Mmag./hoek;
% figure
% plot(hoek,StijfheidPatient,':', hoek, StijfheidMmag, '-.')
% title('stijfheid')
% xlabel('Angle [rad]')
% ylabel('Torque [Nm]')
```

```
%integraal oftewel opp oftewel energie
% energie voor alle magneten opgeteld
totaalenergiemagneet= mean(Mmag)*(max(hoek)-min(hoek))
totaalenergiemagneten= aantalmagneet1*((mean(f1)*(max(x1)-
min(x1))))+aantalmagneet2*((mean(f2)*(max(x2)-
min(x2))))+aantalmagneet3*((mean(f3)*(max(x3)-
min(x3))))+aantalmagneet4*((mean(f4)*(max(x4)-
min(x4)))+aantalmagneet5*((mean(f5)*(max(x5)-min(x5))))
%energy voor magneet op plek 1
totaalenergiemagneet1=
(sum(f1)/((max(hoek)/0.0001)+1))*(max(x1)-min(x1))
%totaalenergiemagneet1Moment=
(sum(M1)/(((max(hoek)/0.0001)+1)))*(max(hoek)-min(hoek))
%dan voor alleen energy van patient
                       (sum(AS2)/((max(hoek)/0.0001)+1))
totaalenergiepatient=
* (max (hoek) -min (hoek))
totaalenergiepatient1= mean(AS2) * (max(hoek)-min(hoek))
% gewicht en efficiency
%work done for 1 magnet
p= [ap1 ap2
                ap3 ap4
                             ap5 ap6
                                           ap7 ap8
                                                           ap9
          ap11];
ap10
q= polyint(p);
a = 0.0;
b = 0.04;
work = diff(polyval(q,[a b]))
work1 = -1*(mean(f4)*((max(x4)-min(x4))))
energyefficiency=
(0.5*(totaalenergiemagneet+totaalenergiemagneten))/((aantalmagn
eet1+aantalmagneet2+aantalmagneet3+aantalmagneet4+aantalmagneet
5) * ((work)))
totaalgewichtmagneet=
                        (aantalmagneet3+
                                            aantalmagneet2
aantalmagneet1+aantalmagneet4+aantalmagneet5) *0.048
energydensity= totaalenergiemagneet/totaalgewichtmagneet
%energyefficiency=
%intf = (1/10)*p1*x.^10 + (1/9)*p2*x.^9 + (1/8)*p3*x.^8
                        (1/6) *p5*x.^6 +
(1/7) *p4*x.^7 +
                                              (1/5) *p6*x.^5
(1/4)*p7*x.^4 + (1/3)*p8*x.^3 + (1/2)*p9*x.^2 + p10*x;
%stijfheid voor magneten
% SM=M1./hoek;
% SM2 = (M2 - M2(1))./hoek;
% SM22= (M2)./hoek;
% SM3 = (M3 - 0.154252523057061)./hoek;
% %SMmag= Mmag./hoek
% AM2 = diff(M2) ;
% AM22 = [M2(1) AM2];
% figure
% plot( hoek, SM2, ':', hoek, M2, hoek, AM22)
% title('Stijfheid magneten')
% xlabel('Angle [rad]')
% ylabel('Torque [Nm]')
% figure
% plot( hoek, AM22)
```

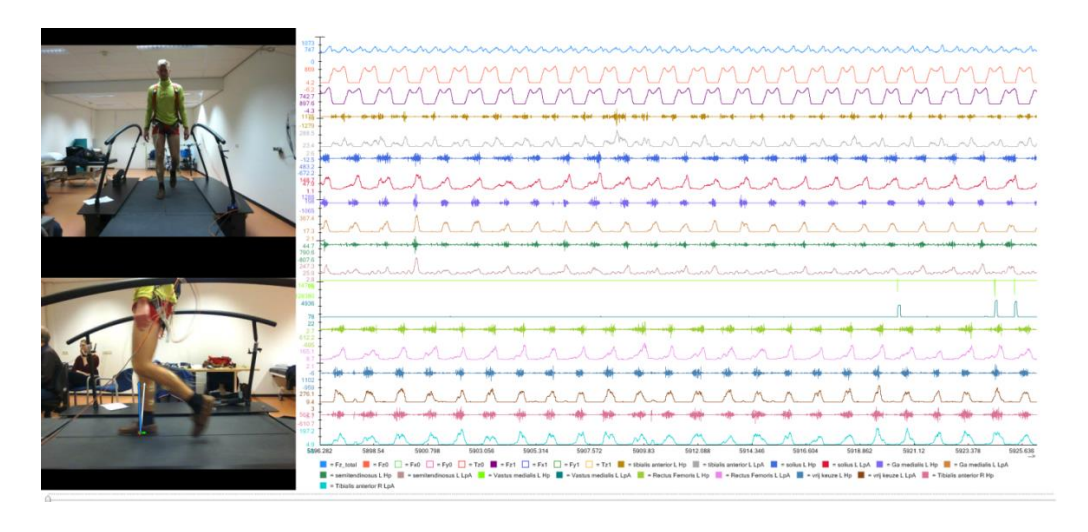
```
% title('Stijfheid magneten')
% xlabel('Angle [rad]')
% ylabel('Torque [Nm]')
% %integraal 1 magneet

z=0:0.0001:0.04;
%Intlmagneet = (1/10)*p1*z.^10 + (1/9)*p2*z.^9 + (1/8)*p3*z.^8
+ (1/7)*p4*z.^7 + (1/6)*p5*z.^6 + (1/5)*p6*z.^5 +
(1/4)*p7*z.^4 + (1/3)*p8*z.^3 + (1/2)*p9*z.^2 + p10*z;
%stijfheid magneet
% figure
% %plot(z,Intlmagneet,x,f)
% title('Stijfheid')
% ylabel('stijfheid [n/m]')
% xlabel('lengte [m]')
```

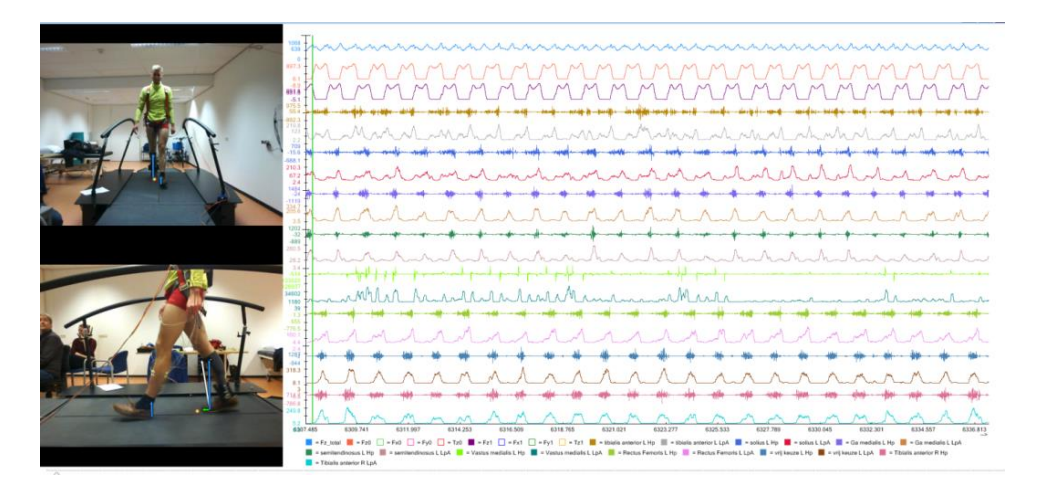
8. Appendix B



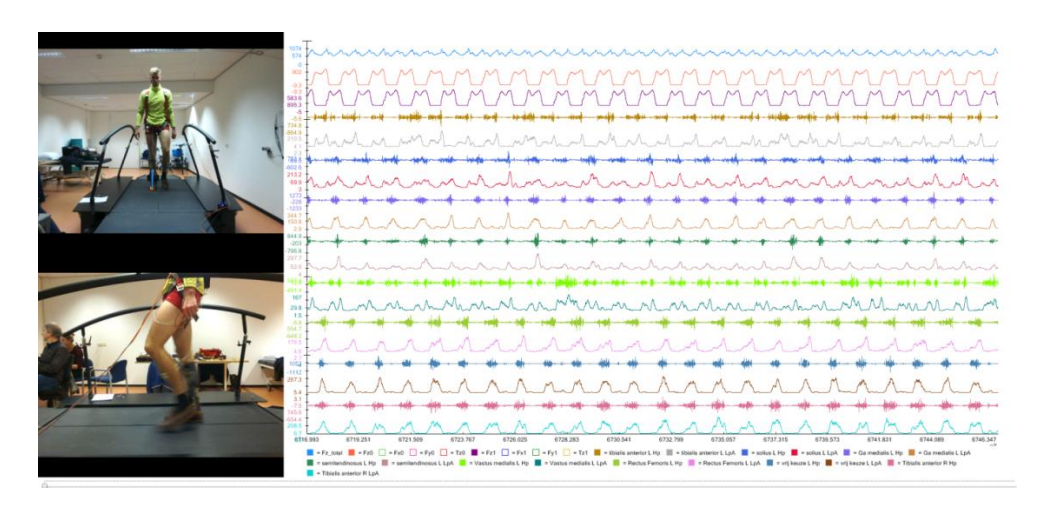
Walking test 0: Bare feet.



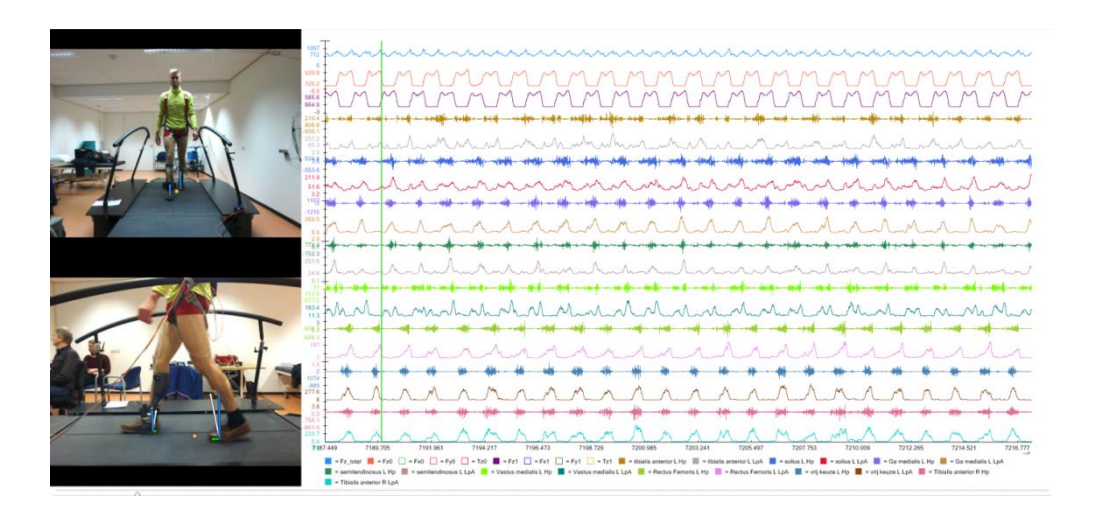
Walking test 1, with shoes.



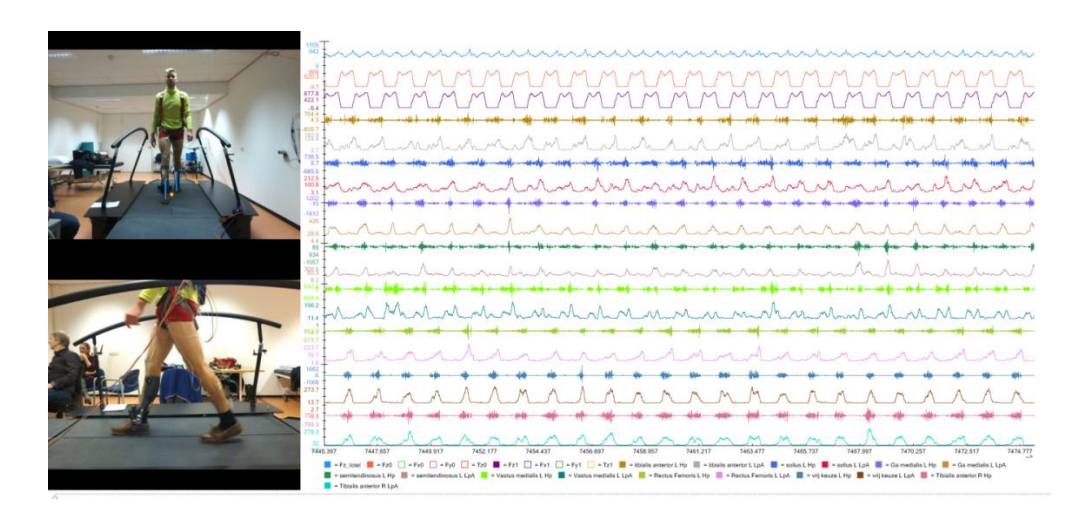
Walking test 2: with NSO without compensation.



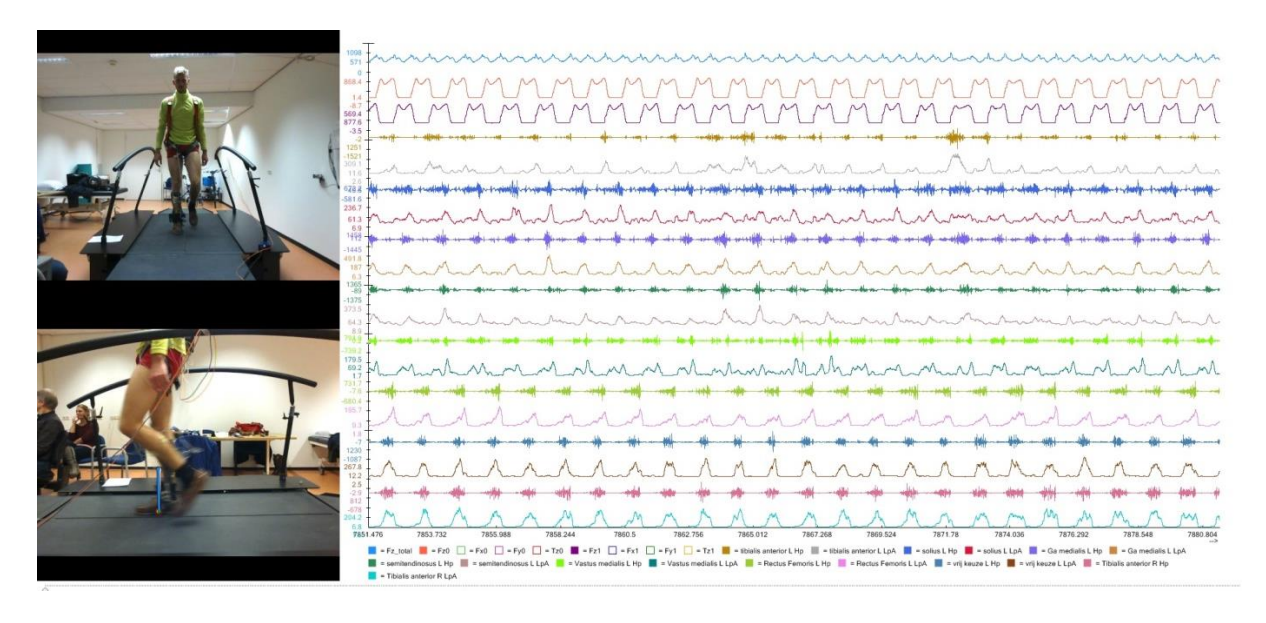
Walking test 3: with NSO with 1 magnet



Walking test 4: with NSO with 2 magnets.



Walking test 5: with NSO with 3 magnets.



Walking test 6: with NSO with 4 magnets.

61